AMERICAN SOCIETY FOR MICROBIOLOGY | mSphere®

RESEARCH ARTICLE

Transcriptional Response of *Candida auris* to the Mrr1 Inducers Methylglyoxal and Benomyl

Amy R. Biermann,[a] Deborah A. Hogan[a]

[a]Department of Microbiology and Immunology, Geisel School of Medicine at Dartmouth, Hanover, New Hampshire, USA

ABSTRACT *Candida auris* is an urgent threat to human health due to its rapid spread in health care settings and its repeated development of multidrug resistance. Diseases that increase risk for *C. auris* infection, such as diabetes, kidney failure, or immunocompromising conditions, are associated with elevated levels of methylglyoxal (MG), a reactive dicarbonyl compound derived from several metabolic processes. In other *Candida* species, expression of MG reductase enzymes that catabolize and detoxify MG are controlled by Mrr1, a multidrug resistance-associated transcription factor, and MG induces Mrr1 activity. Here, we used transcriptomics and genetic assays to determine that *C. auris MRR1a* contributes to MG resistance, and that the main Mrr1a targets are an MG reductase and *MDR1*, which encodes a drug efflux protein. The *C. auris* Mrr1a regulon is smaller than Mrr1 regulons described in other species. In addition to MG, benomyl (BEN), a known Mrr1 stimulus, induces *C. auris* Mrr1 activity, and characterization of the *MRR1a*-dependent and -independent transcriptional responses revealed substantial overlap in genes that were differentially expressed in response to each compound. Additionally, we found that an *MRR1* allele specific to one *C. auris* phylogenetic clade, clade III, encodes a hyperactive Mrr1 variant, and this activity correlated with higher MG resistance. *C. auris MRR1a* alleles were functional in *Candida lusitaniae* and were inducible by BEN, but not by MG, suggesting that the two Mrr1 inducers act via different mechanisms. Together, the data presented in this work contribute to the understanding of Mrr1 activity and MG resistance in *C. auris*.

IMPORTANCE *Candida auris* is a fungal pathogen that has spread since its identification in 2009 and is of concern due to its high incidence of resistance against multiple classes of antifungal drugs. In other *Candida* species, the transcription factor Mrr1 plays a major role in resistance against azole antifungals and other toxins. More recently, Mrr1 has been recognized to contribute to resistance to methylglyoxal (MG), a toxic metabolic product that is often elevated in different disease states. MG can activate Mrr1 and its induction of Mdr1 which can protect against diverse challenges. The significance of this work lies in showing that MG is also an inducer of Mrr1 in *C. auris*, and that one of the major pathogenic *C. auris* lineages has an activating Mrr1 mutation that confers protection against MG.

KEYWORDS Candida auris, Candida, methylglyoxal, benomyl, Mrr1, RNA-seq, transcriptomics

Although *Candida albicans* has historically been the most prominent *Candida* species associated with both superficial and invasive fungal infections, worldwide incidence of non-albicans *Candida* (NAC) species is increasing (1–10). Of particular concern is *Candida auris*, which the CDC classifies as an urgent threat due to its relatively high frequency of resistance to multiple different classes of drugs including amphotericin B, echinocandins, and azoles (reviewed in reference 11). Since its recognition as a novel *Candida* species in 2009, *C. auris*, has been reported in at least 40 countries (12–14).

Editor Aaron P. Mitchell, University of Georgia

Address correspondence to Deborah A. Hogan, dhogan@dartmouth.edu.

The authors declare no conflict of interest.

Received 1 March 2022
Accepted 18 March 2022
Published 27 April 2022

Whole-genome sequencing (WGS) analyses of *C. auris* isolates collected from across the globe indicate the concurrent emergence of four genetically distinct clades (15) with a potential fifth clade defined more recently (16). *C. auris* is thought to primarily colonize the skin (17–19) in addition to a diverse array of body sites, and most clinical isolates to date have been isolated from blood (20). Once *C. auris* has disseminated to the bloodstream, it can cause potentially fatal candidemia which has an estimated global mortality rate ranging from about 30% to 60% (15, 21, 22).

The resistance to azoles in *C. auris* is multifactorial; it has been shown that certain mutations in *ERG11* (15, 23–31) and overproduction of Cdr1 (32–36) contribute to resistance to fluconazole (FLZ). In multiple *Candida* species, the transcriptional regulator Mrr1 also plays a role in FLZ resistance (37–45). Moreover, Mayr and colleagues (46) found three *C. auris* homologs of the transcriptional regulator Mrr1, and showed that one, *MRR1a*, modestly affected fluconazole resistance. Previously, we demonstrated that in *Candida* (*Clavispora*) *lusitaniae*, which is more closely related to *C. auris* relative to other well-studied *Candida* species (12, 47), Mrr1 regulates the expression of *MDR1*, and overexpression of *MDR1* confers resistance to FLZ (40, 48–55), the host antimicrobial peptide histatin-5 (40, 56), bacterially produced phenazines (40), and other toxic compounds (57) in multiple *Candida* species. *C. lusitaniae* Mrr1 also regulates dozens of other genes with two of the most strongly regulated genes encoding methylglyoxal (MG) reductase enzymes, *MGD1* and *MGD2* (37, 40, 58). Mrr1 contributes to *C. lusitaniae* resistance to MG (58), which is a spontaneously formed dicarbonyl electrophile generated as a by-product of several metabolic processes by all living cells (reviewed in reference 59). Via its carbonyl groups, MG reacts non-enzymatically with biomolecules, which can lead to cellular stress and toxicity (reviewed in reference 59). Some of the risk factors (60–69) for candidiasis caused by *C. auris* or other *Candida* spp., such as diabetes (70–72), kidney disease (73–76), or septic shock (77), are associated with elevated MG in human serum. MG resistance across clinical isolates of the same *Candida* species, including *C. auris*, can vary (58).

Through specific regulators, MG and other reactive electrophiles induce stress responses in bacteria (78–80), plants (reviewed in reference 81), mammals (reviewed in reference 82), and the yeasts *Saccharomyces cerevisiae* (83–87) and *Schizosaccharomyces pombe* (88, 89) at subinhibitory concentrations. We found in *C. lusitaniae*, MG induces expression of *MGD1* and *MGD2* as well as *MDR1*, through a mechanism that involved Mrr1 (58), and that MG increased FLZ resistance. *C. auris* displays nosocomial transmission (61–63, 65–69), in part due to its resistance to high temperatures (90) and common surface antiseptics (91), and persistence on abiotic surfaces including latex and nitrile gloves (92), plastics (90), and axillary temperature probes (93). The factors that control *C. auris* stress resistance are not yet known.

In the present study, we show that *C. auris MRR1a* regulates resistance to MG and that MG is an inducer of Mrr1-regulated gene expression. Mrr1a regulates the gene orthologous to the methylglyoxal reductase genes *C. lusitaniae MGD1* in addition to *MDR1*, which regulates FLZ efflux, but the Mrr1a regulon is smaller than that described for other species. Furthermore, we characterize Mrr1a in both clade I and clade III isolates and show that the Mrr1 variant in clade III is constitutively active. Transcriptomics analysis shows that MG elicits a large transcriptional response that is similar in both clade I and clade III, and that there are commonalities in the responses elicited by MG and the Mrr1 inducer benomyl. These data support the model that Mrr1 is a regulator of MG resistance in coordination with efflux proteins such as Mdr1 and provides the basis for future studies on the roles of Mrr1 and MG in survival of *C. auris* in hospital settings.

RESULTS

Mrr1a regulates expression of orthologs to *MDR1* and *MGD1* in *C. auris* strain B11221 and is involved in MG resistance. To determine whether the *C. auris MRR1* orthologs *MRR1a*, *MRR1b*, and *MRR1c* contributed to resistance to MG, we performed growth kinetic assays in yeast extract-peptone-dextrose (YPD) +/– 5 mM, 10 mM, or

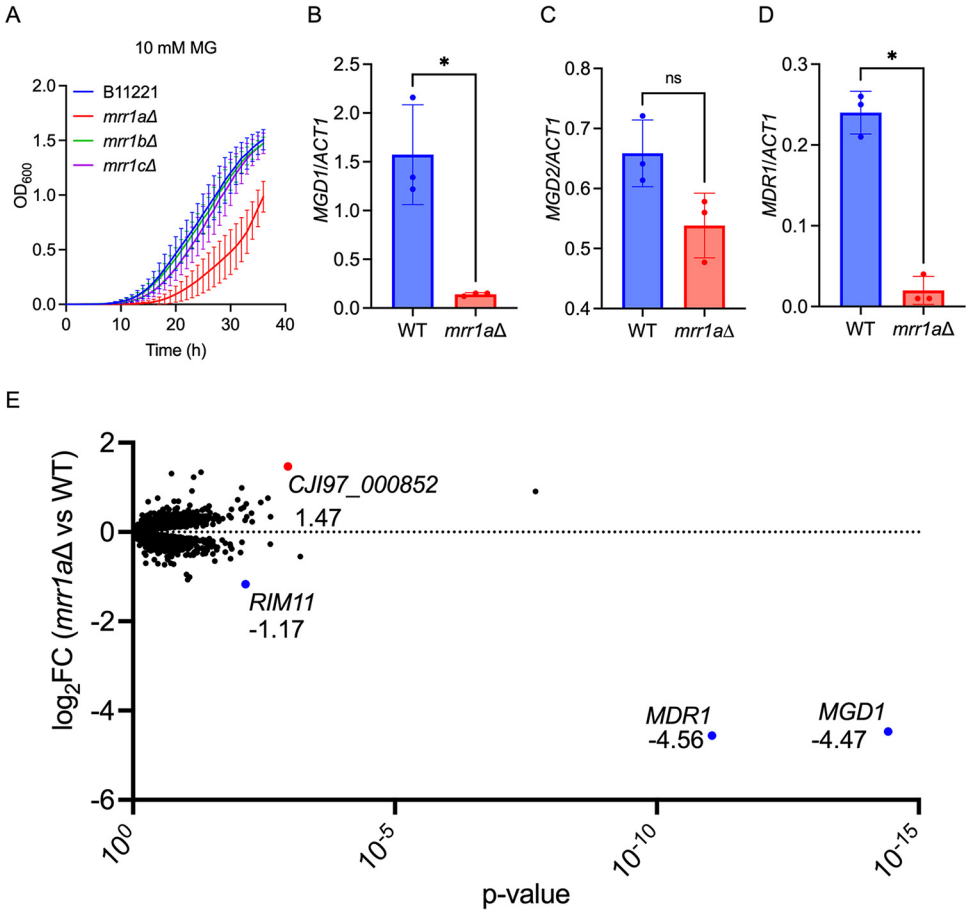

FIG 1 Mrr1a regulates expression of *MGD1* and *MDR1* in *C. auris* isolate B11221. (A) Growth curves of B11221 WT (blue) and its *mrr1a*Δ (red), *mrr1b*Δ (green), and *mrr1c*Δ (purple) derivatives in YPD + 10 mM MG. Data shown represent the mean ± SD for three independent experiments. (B to C) qRT-PCR assessment of *MGD1* (B) and *MDR1* (C) expression in B11221 WT (blue) and *mrr1a*Δ (red) cultures grown to exponential phase in YPD at 37°C. Data shown represent the mean ± SD for three independent experiments. Ratio paired *t* test was used for statistical evaluation; * $P < 0.05$. (D) Volcano plot of all quantified genes in B11221 WT versus *mrr1a*Δ in the control condition. Each point represents a single gene; blue points indicate genes significantly more highly expressed in WT; red points indicate genes significantly more highly expressed in *mrr1a*Δ. Numbers adjacent to each colored point indicate the $\log_2$FC in *mrr1a*Δ versus WT.

15 mM MG. At MG concentrations of 10 mM (Fig. 1A) and 15 mM (Fig. S1), the *mrr1a*Δ mutant displayed a substantial growth defect relative to the parental isolate B11221 (WT), while the *mrr1b*Δ and *mrr1c*Δ mutants exhibited growth comparable to WT. None of the mutants (*mrr1a*Δ, *mrr1b*Δ, or *mrr1c*Δ) differed from the parental isolate B11221 (WT) in YPD alone or in the presence of 5 mM MG (Fig. S1). Like *C. lusitaniae*, the *C. auris* genome encodes multiple putative MG reductases; the closest orthologs to *MGD1* and *MGD2* were *CJI97_000658* and *CJI97_004624*, respectively, in the B11221 genome assembly (58) and we will henceforth refer to these genes as *MGD1* and *MGD2*. For reference, *MGD1* and *MGD2* correspond to *B9J08_000656* and *B9J08_004828*, respectively, in the genome assembly of the *C. auris* reference strain B8441. By quantitative real-time PCR (qRT-PCR), basal expression of *MGD1* was significantly decreased 24-fold in the *mrr1a*Δ mutant relative to B11221 WT (Fig. 1B), and expression of *MGD2* trended lower in the *mrr1a*Δ mutant (~1.2-fold) but this difference did not reach statistical significance (Fig. 1C). *MGD1* was also more highly expressed than *MGD2* in the WT B11221 as in *C. lusitaniae* (58). Consistent with the transcriptional patterns, *C. auris* Mgd1 shares slightly more identity with *C. lusitaniae* Mgd1 than does *C. auris* Mgd2 (63% identity versus 61% identity).

In the *C. auris* B11221 background, expression of *MDR1*, another target of Mrr1 in other species including *C. lusitaniae*, also depended on Mrr1a, as the *mrr1a*Δ mutant

exhibited a significant 21-fold decrease in *MDR1* expression compared to the WT parent (Fig. 1D). These results indicate that in *C. auris MDR1* and *MGD1* are co-regulated, as has been reported in *C. albicans* (44, 45, 94–96), *C. parapsilosis* (97), and *C. lusitaniae* (37, 39, 40, 58, 98), and that higher expression of *MGD1* and/or *MDR1* contributes to growth in high concentrations of MG (Fig. 1A).

In *C. lusitaniae* and other *Candida* species, Mrr1 regulates dozens of genes in addition to *MDR1* and *MGD1* (37, 40). To further elucidate the Mrr1a regulon in *C. auris* isolate B11221, we performed an RNA-seq analysis of in B11221 WT and its *mrr1a*Δ derivative in cells from exponential phase cultures grown at 37°C in YPD. In the control condition (YPD + dH_2O), only four genes, including *MDR1* and *MGD1*, were differentially expressed between the two strains with the cutoff of a $\log_2$ fold change ($\log_2$FC) $\geq$ 1.00 or $\leq$ -1.00 and a *P*-value less than 0.05 (Fig. 1E and Data Set S1 for all data). *MGD1* and *MDR1* showed a 22- and 24-fold decrease, respectively, in *mrr1a*Δ compared with WT, consistent with our qRT-PCR data. *CJI97_005632*, which was 2.25-fold lower in *mrr1a*Δ, is orthologous to the *C. albicans* genes *RIM11* and *C2_04280W_A*, both of which are predicted to encode proteins with serine/threonine kinase activity, though it is worth noting that levels of the transcript were much lower than levels of *MDR1* and *MGD1*. *CJI97_000852*, which was 2.77-fold higher in *mrr1a*Δ than in WT, has 16 orthologs of diverse predicted or known functions in *C. albicans*, including *USO5*, *USO6*, and *RBF1* (Fig. 1E and Data Set S1). Notably, *MGD2* was not differentially expressed between B11221 WT and the *mrr1a*Δ mutant in our RNA-seq data (Data Set S1), consistent with our qRT-PCR results described above.

Mrr1a regulates only *MDR1* and *MGD1* in response to MG and benomyl. We have previously shown in *C. lusitaniae* that MG induces expression of the Mrr1-regulated genes *MGD1* and *MGD2* in an Mrr1-dependent manner, and *MDR1* in a partially Mrr1-dependent manner (58). To determine if MG would induce expression of *MGD1*, *MGD2*, and/or *MDR1* in *C. auris*, we purified RNA for qRT-PCR from exponential-phase cultures of B11221 WT and *mrr1a*Δ treated with 5 mM MG or an equal volume of dH_2O for 15 min. We found that MG treatment significantly enhanced expression of *MGD1* in WT by 2.4-fold but not in *mrr1a*Δ (Fig. 2A). *MGD1* was also induced by a 30-min treatment with 25 μg/mL benomyl (BEN), a known inducer of Mrr1-regulated genes in other *Candida* species (37, 41, 43, 95, 99–104), by 7.5-fold in the WT (Fig. 2A). The different treatment times for MG and BEN were used to be consistent with previous studies using either compound in the related species *C. lusitaniae* (37, 58). Expression of *MDR1* was also more highly induced by treatment with either MG or BEN in WT compared with the *mrr1a*Δ mutant by 6- and 14.5-fold, respectively (Fig. 2B). Although *MDR1* expression was significantly induced by MG and BEN in the *mrr1a*Δ, transcript levels of *MDR1* were approximately 20-fold higher in the WT than in the *mrr1a*Δ under these conditions (Fig. 2B), suggesting that Mrr1a is required for maximum expression of *MDR1* in response to stimuli.

To describe the complete Mrr1-dependent MG- and BEN-response regulon under our test conditions in *C. auris*, we also performed RNA-seq on exponential-phase cultures of B11221 WT and *mrr1a*Δ treated with MG or BEN as described above. In B11221 WT, MG led to the upregulation of 319 genes and downregulation of 133 genes compared with the control condition (Fig. 2C and Data Set S1). In the *mrr1a*Δ mutant, MG led to the upregulation of 349 genes and downregulation of 143 genes compared with the control condition (Fig. S2A and Data Set S1). Consistent with our qRT-PCR data in Fig. 2A, MG induced expression of *MGD1* in the WT but not in the *mrr1a*Δ mutant (Table S1 and Data Set S1). Although expression of *MDR1* was significantly induced by MG in both the WT and the *mrr1a*Δ mutant (Table S1 and Data Set S1), levels of *MDR1* were substantially lower in the *mrr1a*Δ mutant even in the presence of MG (Fig. 2D and Data Set S1), also in agreement with our qRT-PCR data. *MGD1* and *MDR1* strongly stood out as the only two genes in the MG response that were strongly dependent on Mrr1a (Fig. 2D).

Treatment with BEN led to upregulation of 160 genes and downregulation of 163 genes in the WT (Fig. 2E and Data Set S1). In the *mrr1a*Δ mutant, 181 genes were

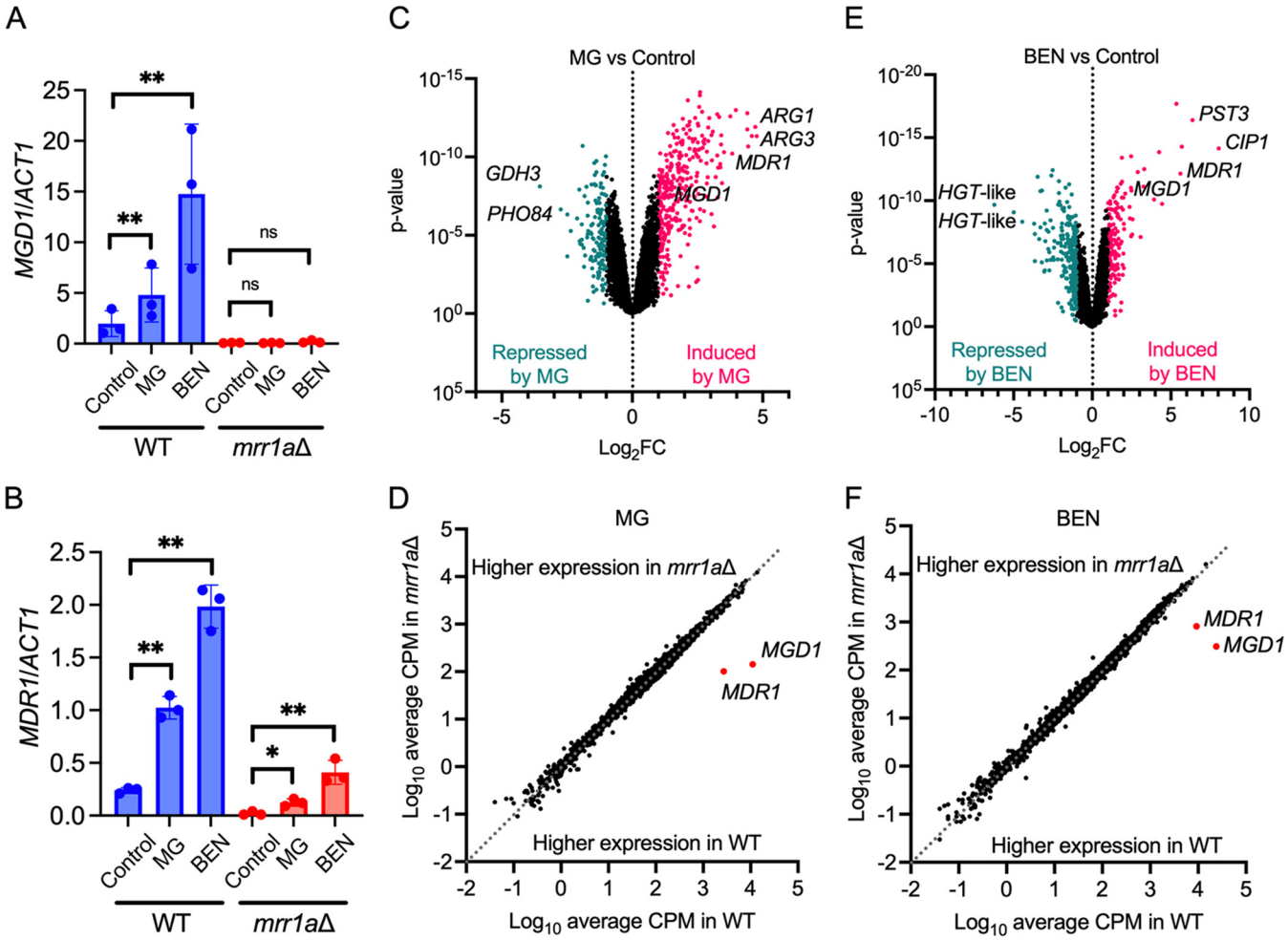

FIG 2 MG and BEN both lead to a vast transcriptional response in *C. auris* B11221, which includes upregulation of *MDR1* and *MGD1*. (A to B) qRT-PCR analysis for expression of *MGD1* (A) and *MDR1* (B) in exponential-phase cultures of B11221 WT (blue) or *mrr1a*Δ (red) treated with MG or BEN as indicated. Data shown represent the mean ± SD for three independent experiments. Ratio paired *t* test was used for statistical evaluation; ns $P > 0.05$; * $P < 0.05$; ** $P < 0.01$. (C to D) Volcano plots of all quantified genes in B11221 WT treated with either MG (C) or BEN (D). Each point represents a single gene; magenta points indicate genes that were significantly upregulated compared with the control condition, teal points indicate genes that were significantly downregulated compared to the control condition. *MDR1* and *MGD1* are shown along with the two most up- and downregulated genes in each condition. (E to F) Scatterplots of the average CPMs of all quantified genes in *mrr1a*Δ versus B11221 WT treated with MG (E) or BEN (F). Each point represents a single gene. Points below the dotted line indicate genes that were more highly expressed in the WT, and points above the dotted line indicated genes that were more highly expressed in the *mrr1a*Δ mutant. *MDR1* and *MGD1* are shown with red dots for reference.

upregulated, and 229 genes were downregulated in response to BEN (Fig. S2B and Data Set S1). Like MG, induction of *MGD1* by BEN was completely dependent on Mrr1a (Table S1 and Data Set S1) and *MGD2* expression was not induced by BEN (Data Set S1). Expression of *MDR1* was also induced by BEN in both the WT and the *mrr1a*Δ mutant, but as with MG, *MDR1* levels in the *mrr1a*Δ mutant did not reach that of the WT even with BEN treatment (Fig. 2F and Data Set S1). Again, *MGD1* and *MDR1*, appear to be the only genes in *C. auris* whose induction of expression by either MG or BEN is dependent on Mrr1a. The Mrr1a-independent responses to MG and BEN are discussed further below.

B11221 has higher basal expression of *MDR1* and of putative MG reductase genes compared with the clade I isolate AR0390. Many clade III isolates, including B11221, contain an N647T single nucleotide polymorphism (SNP) in *MRR1a* (25, 105). In Iyer et al., this SNP was proposed to be a gain-of-function mutation due to the resistance of clade III isolates against azoffluxin, a novel antifungal compound that inhibits expression and activity of *C. auris* efflux pumps (105). As a first step to determine whether there were differences in activity between the Mrr1a protein encoded by the N647T allele found in clade III and the variant encoded by the allele found in clades I, II, and IV, we

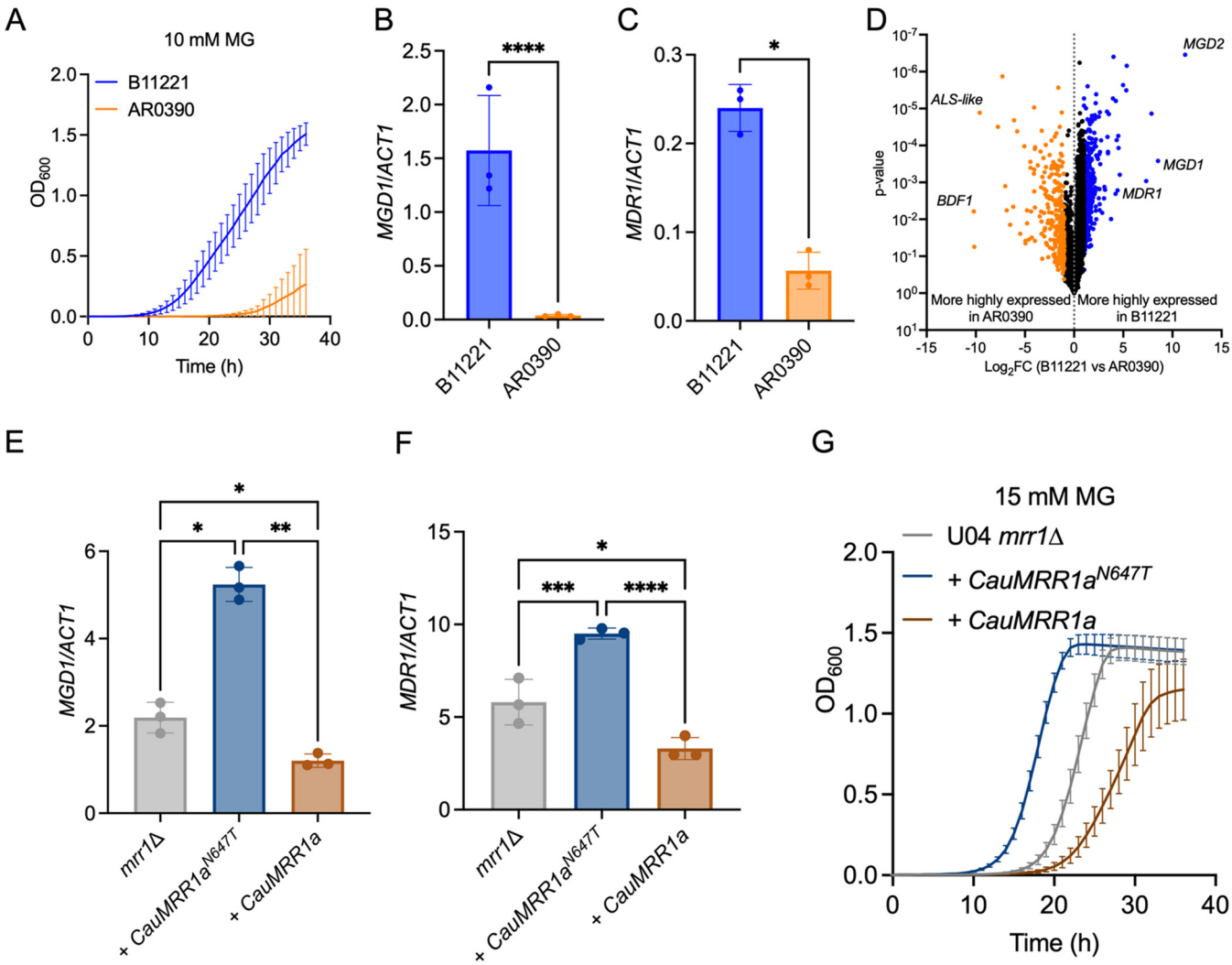

FIG 3 *MDR1* and *MGD1* are among the genes significantly more highly expressed in isolate B11221 compared with isolate AR0390. (A) Growth curves of B11221 (blue) and AR#0390 (orange) in YPD + 10 mM MG. Data shown represent the mean ± SD for three independent experiments. (B to C) qRT-PCR assessment of *MGD1* (B) and *MDR1* (C) expression in B11221 (blue) and AR0390 (orange) grown to exponential phase in YPD at 37°C. Data shown represent the mean ± SD for three independent experiments. Ratio paired *t* test was used for statistical evaluation; * $P < 0.05$; **** $P < 0.0001$. (D) Volcano plot of all quantified genes, matched by syntenic ortholog, in B11221 and AR0390 in the control condition (YPD). Each point represents a single gene; blue points indicate genes significantly more highly expressed in B11221; orange points indicate genes significantly more highly expressed in AR0390. (E to F) qRT-PCR expression analysis for *MGD1* (E) and *MDR1* (F) in *C. lusitaniae* U04 *mrr1*Δ (gray) and its derivatives expressing *CauMRR1a*^{N647T} (dark blue) or *CauMRR1a* (brown). Data shown represent the mean ± SD for three independent experiments. One-way ANOVA was used for statistical evaluation; * $P < 0.05$; ** $P < 0.01$; *** $P < 0.001$; **** $P < 0.0001$. (G) Growth curves of *C. lusitaniae* U04 *mrr1*Δ (gray) and its derivatives expressing *CauMRR1a*^{N647T} (dark blue) or *CauMRR1a* (brown) in YPD + 15 mM MG. One representative experiment of three independent experiments is shown; error bars represent the standard deviation of technical replicates within the experiment.

compared MG sensitivity of B11221 to that of clade I isolate AR0390. Interestingly, AR0390 grew substantially better than B11221 in the YPD control but showed a greater reduction in growth in YPD with 5 mM MG than did B11221 (Fig. S3). At concentrations of 10 mM (Fig. 3A) and 15 mM MG (Fig. S3), AR0390 exhibited a profound growth defect compared with B11221. To determine if differences in MG sensitivity were due to differences in *MGD1* expression, we measured basal expression of *MGD1* and its co-regulated gene *MDR1* in B11221 and AR0390 using qRT-PCR. Both genes were significantly more highly expressed in B11221 by 42- and 4.2-fold, respectively (Fig. 3B and C).

To gain a deeper understanding of the broader transcriptional differences between B11221 and AR0390, we compared the basal global gene expression in YPD of the two strains using RNA-seq. First, we matched the 5,227 syntenic orthologs between the genomes of B11221 and the clade I reference strain B8441 to compare expression of each gene under the control condition. Of these, 755 genes were differentially expressed

between B11221 and AR0390 in the control condition ($|\log_2 FC| \geq 1.00$, FDR-corrected $P < 0.05$) (Fig. 3D, Data Set S1). The top 20 differentially expressed genes whose orthologs have known or predicted functions in *C. albicans* are reported in Table S2. Strikingly, the two genes which exhibited the largest difference in expression between B11221 and AR0390 were *MGD2* ($\log_2 FC = 11.29$) and *MGD1* ($\log_2 FC = 8.53$) (Fig. 3D, Table S2, and Data Set S1). A third gene with homology to MG reductases, *CJI97_001800/B9J08_002257*, was also more highly expressed in B11221, although the $\log_2 FC$ in expression of this gene in B11221 versus AR0390 was only 1.41 (Data Set S1). Low expression of *MGD1*, *MGD2*, and/or *B9J08_002257* may contribute to the severe growth defect of AR0390 in the presence of MG. Consistent with our qRT-PCR data, *MDR1* was also significantly more highly expressed in B11221 relative to AR0390 ($\log_2 FC = 4.42$) (Fig. 3D and Table S2). Although *MGD2* and *B9J08_002257* do not appear to be regulated by Mrr1a in our studies, it is nonetheless interesting to note the elevated expression of three putative MG reductases in the *MDR1*-overexpressing *C. auris* isolate B11221, as the co-expression of *MDR1* with at least one MG reductase has been reported in numerous studies in other *Candida* species (37, 40, 44, 45, 58, 94–97).

Clade III Mrr1a^{N647T} exhibits a gain-of-function phenotype compared with clade I Mrr1a when expressed in *C. lusitaniae*. To compare the activities of the proteins encoded by the *MRR1a* alleles of B11221 and AR0390 more directly, we heterologously expressed each allele, henceforth referred to as *CauMRR1a^{N647T}* and *CauMRR1a*, respectively, independently in a *C. lusitaniae mrr1*Δ mutant previously generated and characterized by our lab (37, 40, 58). All three *C. lusitaniae* clones expressing *CauMRR1a^{N647T}* which we tested exhibited a 4-fold increase in FLZ MIC relative to the U04 *mrr1*Δ parent (16 μg/mL versus 4 μg/mL), confirming that *C. auris* clade III *MRR1a* can complement *MRR1*-dependent FLZ resistance in *C. lusitaniae* and adding support to the hypothesis that the N647T substitution in clade III *MRR1a* confers increased activity. However, the FLZ MIC of the three tested *C. lusitaniae* clones expressing *CauMRR1a* did not differ from that of U04 *mrr1*Δ (4 μg/mL), so FLZ MIC alone could not indicate whether this allele is functional in *C. lusitaniae*. One clone expressing each *C. auris MRR1a* allele was chosen at random for the remaining experiments described in this paper: clone #1 for *CauMRR1a^{N647T}* and clone #5 for *CauMRR1a*. Using qRT-PCR, we then examined basal expression levels of *C. lusitaniae MGD1* (*CLUG_01281*) and *MDR1* (*CLUG_01938/CLUG_01939*) in the heterologous complements and the U04 *mrr1*Δ parent. Complementation with *CauMRR1a^{N647T}* conferred a significant increase in basal expression of both *MGD1* (Fig. 3E) and *MDR1* (Fig. 3F) compared with the *mrr1*Δ parent, while complementation with *CauMRR1a* led to a small, but significant, decrease in expression of both genes relative to *mrr1*Δ (Fig. 3E and F). These results are consistent with our previous observations that *C. lusitaniae* strains expressing certain Mrr1 variants with low basal activity demonstrate lower expression of some Mrr1-regulated genes, including *MDR1* and *MGD1*, compared with an isogenic *mrr1*Δ strain suggesting that Mrr1 has both repressing and activating roles (37, 58). Finally, we assessed the relative MG resistance of the isogenic *C. lusitaniae* strains expressing *CauMRR1a^{N647T}* or *CauMRR1a* and the U04 *mrr1*Δ parent. The *CauMRR1a^{N647T}* complement grew markedly better in 15 mM MG compared with U04 *mrr1*Δ whereas the *CauMRR1a* complement grew substantially worse than U04 *mrr1*Δ (Fig. 3G), consistent with the pattern of *MGD1* expression we observed in these strains via qRT-PCR. None of the *C. lusitaniae* strains demonstrated growth differences in the YPD control, or in the presence of MG at concentrations of 5 mM or 10 mM (Fig. S4).

MG induces expression of *MGD1* and *MDR1* in *C. auris* B11221 and AR0390, but not in *C. lusitaniae* strains expressing *C. auris MRR1a* alleles. Next, we compared induction of *MGD1* and *MDR1* by MG in the *C. auris* strains B11221 and AR0390 via qRT-PCR. MG significantly induced expression of *MGD1* by 2.4-fold in *C. auris* strain B11221 and by 4.0-fold in *C. auris* strain AR0390 (Fig. 4A) and expression of *MDR1* by 6.0-fold in B11221 and 9.3-fold in AR0390 (Fig. 4B). AR0390 displayed lower expression of both genes in MG, but a higher fold change compared to B11221, further supporting the hypothesis that the N647T allele is gain-of function.

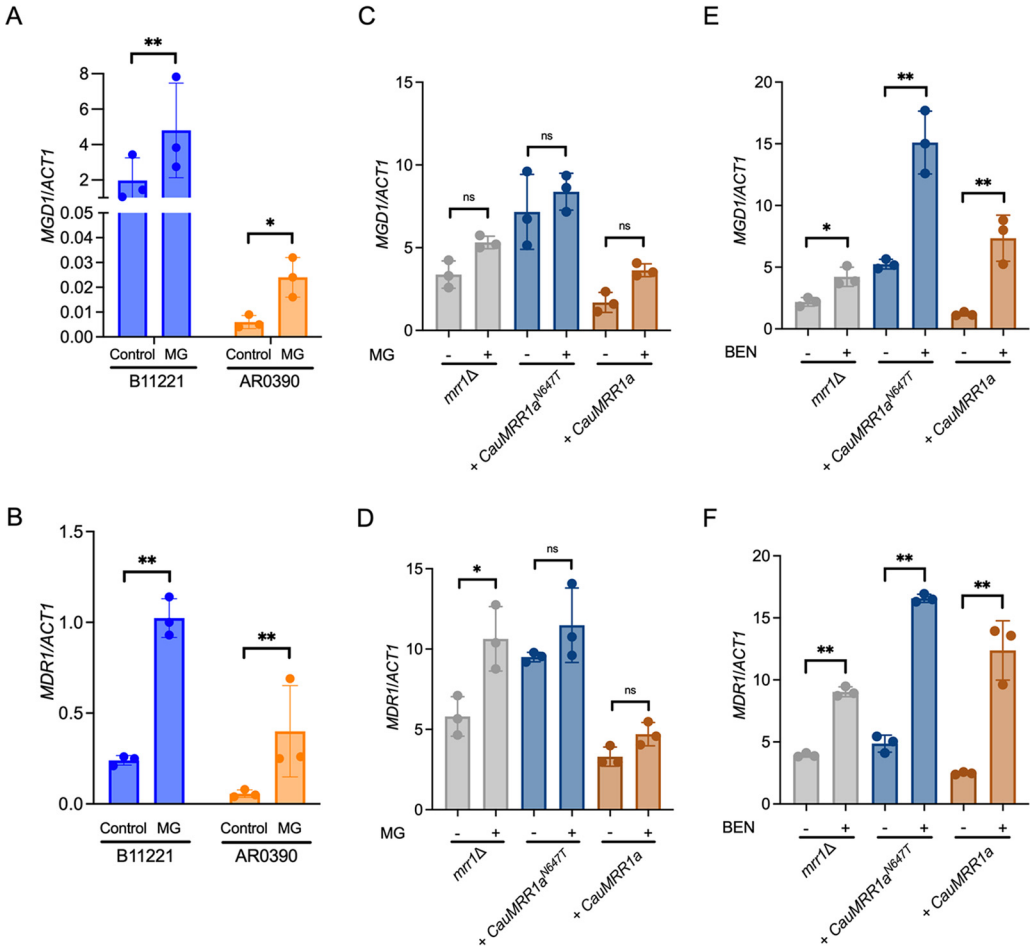

FIG 4 MG induces expression of *MGD1* and *MDR1* in *C. auris* isolates B11221 and AR0390, but *C. auris MRR1a* is not inducible by MG when heterologously expressed in *C. lusitaniae*. (A to B) qRT-PCR analysis for expression of *MGD1* (A) and *MDR1* (B) in exponential-phase cultures of B11221 (blue) or AR0390 (orange) treated with MG as indicated. Data shown represent the mean ± SD for three independent experiments. Ratio paired *t* test was used for statistical evaluation; ns $P > 0.05$; * $P < 0.05$; ** $P < 0.01$. (C to F) qRT-PCR analysis for expression of *MGD1* (C, E) and *MDR1* (D, F) in exponential-phase cultures of *C. lusitaniae* U04 *mrr1*Δ (gray) and its derivatives expressing *CauMRR1a*^{N647T} (dark blue) or *CauMRR1a* (brown) treated with 5 mM MG for 15 min (C, D) or 25 μg/mL BEN for 30 min (E, F). Data shown represent the mean ± SD for three independent experiments. Ratio paired *t* test was used for statistical evaluation; ns $P > 0.05$; * $P < 0.05$; ** $P < 0.01$.

Finally, we compared induction of *MGD1* and *MDR1* by MG in the isogenic *C. lusitaniae* strains expressing either *CauMRR1a*^{N647T} or *CauMRR1a* and the *mrr1*Δ parent. Additionally, we tested induction by BEN in these strains as a control. While the *mrr1*Δ parent exhibited a significant 1.8-fold induction of *MDR1*, neither *C. lusitaniae* strain expressing a *C. auris* Mrr1a allele demonstrated a significant change in *MGD1* or *MDR1* expression in response to MG (Fig. 4C and D), indicating that *C. auris* Mrr1a may repress *MRR1*-independent MG induction of *MDR1* in *C. lusitaniae* and that induction of *MGD1* by MG in *C. lusitaniae* requires a functional *MRR1* allele from its own species. Treatment with BEN led to significant increase in expression of *MGD1* (Fig. 4E) and *MDR1* (Fig. 4F) in all three *C. lusitaniae* strains. In response to BEN, *MGD1* was induced by 1.9-fold in *mrr1*Δ, 2.9-fold in the *CauMRR1a*^{N647T} complement, and 6.1-fold in the *CauMRR1a* complement (Fig. 4E). Likewise, expression of *MDR1* was induced by 2.3-fold in *mrr1*Δ, 3.5-fold in the *CauMRR1a*^{N647T} complement, and 5.0-fold in the *CauMRR1a* complement in response to BEN (Fig. 4F). The striking difference in the ability of the *C. lusitaniae* strains expressing *C. auris MRR1a* alleles to respond to BEN versus MG suggests that there are differences in the mechanisms by which BEN and MG induce Mrr1-dependent transcriptional activation and that MG induction of *C. auris* Mrr1a is not supported by *C.*

lusitaniae factors. These potential differences are a topic of future study and may shed light on mechanisms of Mrr1 activation in *Candida* species.

MG and BEN induced Mrr1a-independent transcriptional responses in *C. auris*. We have previously observed heterogeneity in MG resistance as well as MG-induced FLZ resistance among several *C. auris* isolates from different clades (58), and thus we were interested in whether the overall transcriptional response to MG was more similar or different in B11221 and AR0390. AR0390 had greater number of genes differentially expressed by MG compared with B11221; 438 genes were significantly upregulated, and 242 genes were significantly downregulated by MG (see Fig. S5 for the volcano plot of all genes). More genes had a larger fold change in response to MG in AR0390 compared with B11221, including *MGD1* and *MDR1* (Fig. 5A), consistent with the qRT-PCR results in Fig. 4A and B. However, there was a large overlap of 254 genes which were induced by MG in both strains (Fig. 5B), suggesting a common response across these two genetically distinct clades. These commonly induced genes include many with putative roles in amino acid biosynthesis; transmembrane transport; or acquisition and usage of sulfur (Fig. 5C and Table S3). The complete comparison is available in Data Set S1.

Only 68 genes with syntenic orthologs across both strains were commonly repressed by MG (Fig. 5B). These genes include some with putative roles in metal transport or carbohydrate uptake and metabolism (Fig. 5C and Table S3). We did not observe obvious patterns in genes that were only induced or repressed in one strain, and some genes that are listed as only induced or repressed in one strain were close to the cutoff in the other strain.

The groups of genes that were differentially expressed in response to MG in both B11221 and AR0390 were also evident in the response of B11221 to BEN as well as the response of the *mrr1a*Δ mutant in response to MG and BEN. In B11221, a total of 46 genes exhibited significant induction by both MG and BEN, including *MGD1* and *MDR1*. Many of the 44 other genes have predicted roles in assimilation and biosynthesis of sulfur-containing compounds or xenobiotic transport (Fig. 5C and Table S1). MG also induced expression of many genes with predicted roles in the biosynthesis of amino acids. The two genes most highly upregulated upon MG treatment, in terms of fold change, in this strain were orthologous to the arginine biosynthesis genes *ARG3* ($\log_2$FC = 4.77) and *ARG1* ($\log_2$FC = 4.72) (Fig. 2C and Table S1). Conversely, BEN had a limited effect on expression of amino acid biosynthesis genes (Table S1). There were also common themes among the genes that were significantly repressed by both MG and BEN in B11221. Genes that were repressed by both MG and BEN included four orthologs of the *HGT* glucose transporter family, five genes with a predicted role in uptake of iron and/or copper, and *ERG6*, which encodes an enzyme in the ergosterol biosynthesis pathway (Fig. 5C and Table S1). The genes that were repressed by only one stimulus, MG or BEN, also included those involved in ergosterol biosynthesis and the uptake of iron, copper, or glucose (Fig. 5C, Table S1). In general, the transcriptional response of the *mrr1a*Δ mutant to MG and BEN was similar to that of B11221 WT (Fig. S2 and Table S1). The complete data sets for MG and BEN responses are available in Data Set S1.

DISCUSSION

In this work, we have demonstrated that in *C. auris*, the zinc-cluster transcription factor Mrr1a, which is orthologous to Mrr1 in other *Candida* species, strongly regulates expression of a putative MG reductase *MGD1* in addition to *MDR1*, and that Mrr1a plays a role in MG resistance, highlighting a function of Mrr1 that is distinct from antifungal resistance. We also compared basal global gene expression in B11221 and AR0390 and found that *MDR1*, *MGD1*, and *MGD2* were among the genes significantly more highly expressed in B11221, consistent with the higher MG resistance of this isolate relative to AR0390. These differences were explained by our finding that *MRR1a* from B11221 encoded a higher activity variant than that from AR0390 as evidenced by a higher FLZ

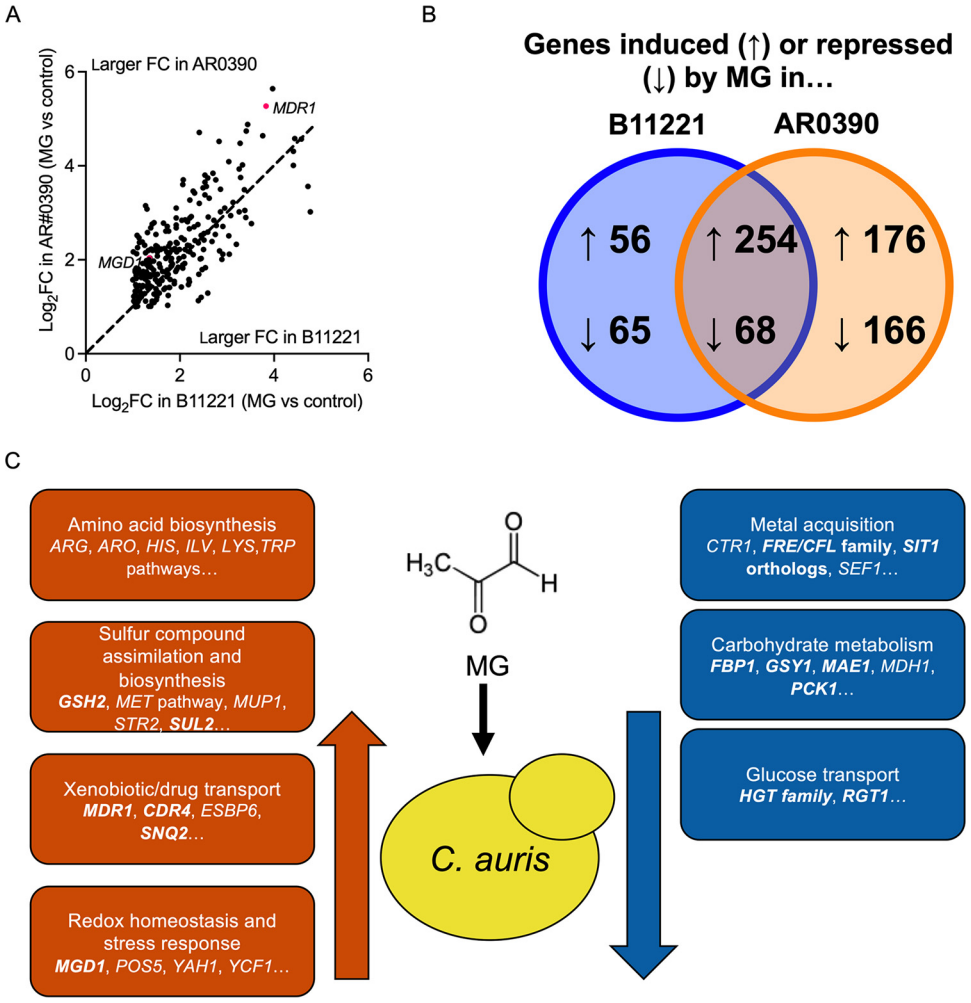

FIG 5 MG induces and represses common pathways across B11221 and AR0390. (A) Venn diagram of genes with syntenic orthologs between B11221 and AR0390 that were significantly induced (indicated by "up" arrows) or repressed (indicated by "down" arrows) by MG in either or both strains. (B) Scatterplot of the $\log_2$FC of genes significantly induced by MG in AR0390 versus the $\log_2$FC of genes induced by MG in B11221. Only genes with syntenic orthologs between the two strains are shown. Each point represents a single gene; points above the dotted line indicate genes which exhibited a greater Log_2FC in AR0390, and points below the dotted line indicate genes which exhibited a greater $\log_2$FC in B11221. *MGD1* and *MDR1* are indicated with red dots for reference. (C) Graphic summary of major groups of genes that were significantly up- or downregulated in response to MG in both B11221 and AR0390. Genes in bold text were also up- or downregulated in response to BEN in B11221.

MIC, higher expression of *MDR1* and *MGD1*, and higher MG resistance in the strain expressing *CauMRR1a*^{N647T} compared with the isogenic strain expressing *CauMRR1a*. The allele from B11221 contains an N647T amino acid substitution (25, 105) which is in the central region of the regulator where other gain of function substitutions have been found. Both alleles result in induction of *MDR1* and *MGD1* in response to BEN but not to MG in *C. lusitaniae*, suggesting that these two compounds activate Mrr1-dependent transcription through different mechanisms.

Under the conditions tested, Mrr1a regulation in the *C. auris* B11221 background was mainly of *MGD1* and *MDR1*. Homologs of *MDR1* and at least one gene encoding a known or predicted MG reductase are co-regulated by Mrr1 in *C. albicans* (44, 45, 94–96), *C. parapsilosis* (97), and *C. lusitaniae* (37, 40, 58), suggesting that the co-regulation of these two genes has been conserved throughout multiple *Candida* species. Gaining a deeper understanding of the evolutionary and biochemical relationship between methylglyoxal reductases and efflux pumps, particularly Mdr1, may shed light on how

Candida species sense and respond to environmental or physiological stresses, evade host defense mechanisms, and develop antifungal resistance. In all other *Candida* species with published Mrr1 regulons, however, Mrr1 appears to regulate expression of many more genes than the four we have described here in the *C. auris* strain B11221 (37, 40, 44, 45, 97). The surprisingly small number of *C. auris* genes whose expression was significantly altered by genetic deletion of *MRR1a* may be due to possible redundancy between *MRR1a* and the other two *MRR1* orthologs in *C. auris*, *MRR1b*, and *MRR1c*, although further studies would be necessary to test this hypothesis. It is striking, however, that *MRR1a* alone seems to be necessary for expression and induction of *MGD1*, which is further supported by our observation that only the *mrr1a*Δ mutant had a growth defect in MG compared with parental B11221 (Fig. 1A).

Our demonstration of increased basal activity of the *CauMRR1a*^{N647T} allele compared with the allele from AR0390 supports the hypothesis put forth by Iyer et al. (105) that the N647T substitution found in many clade III isolates is a gain-of-function mutation. Furthermore, this may explain why deletion of *MRR1a* leads to a mild decrease in azole resistance in B11221, but not in the clade IV isolate B11243 (46). In *C. albicans*, knocking out gain-of-function *MRR1* causes a significant decrease in FLZ resistance, but knocking out *MRR1* with wild-type transcriptional activity does not alter FLZ resistance (41, 44, 45, 106). Similarly, knocking out gain-of-function *MRR1* in *C. lusitaniae* also decreases FLZ resistance, although knocking out *MRR1* alleles that do not encode a constitutively active protein generally leads to increased FLZ resistance (37).

Although Mrr1a does not appear to play a major role in *C. auris* azole resistance (46), our findings suggest that it contributes to resistance against MG, which may be encountered in the host environment. We have previously shown that Mrr1 also contributes to MG resistance in *C. lusitaniae* in a manner that is partially dependent on *MGD1* and *MGD2* (58). Indeed, gain-of-function mutations in *MRR1* may arise in various *Candida* species due to selective pressures other than azoles. In *C. lusitaniae*, we have reported the emergence of gain-of-function mutations in *MRR1* among isolates from a patient with no history of clinical antifungal use (40). In *C. auris*, most sequenced clade III isolates exhibit both the *MRR1a*^{N647T} allele and the *ERG11*^{F126L} allele (25), the latter of which has been shown to be a major contributor to azole resistance (31). Although it is not known whether the *MRR1a* or *ERG11* mutation occurred first in the clade III lineage, it seems plausible that if the *ERG11* mutation did occur first, evolution of the *MRR1a*^{N647T} allele in *C. auris* is likely to be the result of selection for *MGD1* expression and/or an unknown role for Mdr1 that is unrelated to azole resistance. Therefore, we hypothesize that Mrr1 may act, either directly or indirectly, as a response regulator for carbonyl stress in *Candida* species, and future studies will investigate a possible role for Mrr1 in resistance against other physiologically relevant reactive carbonyl compounds.

Curiously, although both variants of *C. auris* Mrr1a were inducible by BEN when expressed in *C. lusitaniae*, they were not inducible by MG under the conditions tested (Fig. 4E and F). One possible hypothesis for this observation is that Mrr1 must interact with at least one particular binding partner to induce transcription in response to MG, and that *C. auris* Mrr1a does not bind efficiently to this *C. lusitaniae* Mrr1-binding protein or complex. Differential requirements for Mrr1-dependent transcriptional activation by chemical stressors have reported in *C. albicans*. For example, the transcription factor Mcm1 is required for Mrr1-dependent induction of *MDR1* in response to BEN but not to H_2O_2 (101), and the redox-sensing transcription factor Cap1 is required for *MDR1* induction by H_2O_2 and may play a role in *MDR1* induction by BEN (44). Furthermore, gain-of-function Mrr1 in *C. albicans* requires the Swi/Snf chromatin remodeling complex to maintain promoter occupancy, and the kinase Ssn3, which is a subunit of the Mediator complex, may act in opposition to Mrr1 or its coactivators (38). Thus, although *C. auris* Mrr1a can complement Mrr1-dependent basal and BEN-induced expression of *MDR1* and *MGD1* in *C. lusitaniae*, it may be incompatible with certain elements of the *C. lusitaniae* MG-responsive transcriptional machinery. Further studies on

the differences between *C. lusitaniae* and *C. auris* Mrr1, particularly in the presence of MG, may elucidate more detailed mechanisms of Mrr1 activation.

In general, we observed substantial upregulation of genes with predicted roles in transmembrane transport, sulfur metabolism, and amino acid biosynthesis in response to MG in all three strains tested. Many genes downregulated in response to MG in all three strains have predicted roles in metal acquisition, particularly iron, and carbohydrate metabolism. In both B11221 WT and *mrr1a*Δ, BEN treatment led to differential expression of similar groups of genes as MG in addition to induction of genes with predicted roles in oxidative stress response. Our studies of the transcriptional response of *C. auris* to MG and BEN contribute to the understanding of how *Candida* species may adapt to oxidative and/or carbonyl stress, two types of stress that a pathogen is likely to encounter in the host environment. In humans, elevated serum MG has been reported in diabetes as well as in renal failure, which are both risk factors for *Candida* infection (107, 108). There is also evidence that neutrophils (109) and macrophages (110, 111) generate MG during the inflammatory response, consistent with elevated levels of MG in sepsis patients (77). In our transcriptomics analysis of three *C. auris* strains exposed to 5 mM MG for 15 min, upregulation of numerous genes involved in amino acid uptake, metabolism, and biosynthesis was one of the most striking responses to MG (Table S1 for comparison of MG and BEN in B11221 WT and *mrr1a*Δ and Table S2 for the comparison of genes induced by MG in B11221 and/or AR0390). In particular, induction of *ARG* genes is interesting considering the report that *C. albicans* upregulates expression of arginine biosynthesis genes when phagocytosed by macrophages or in response to sublethal concentrations of hydrogen peroxide, tert-butyl hydroperoxide, or menadione *in vitro* (112). This induction of *ARG* genes in *C. albicans* by macrophages is dependent on the $gp91^{phox}$ subunit of the macrophage oxidase, and thus is likely a direct response to oxidative stress rather than arginine depletion (112). In our data set, *ARG3* and *ARG1* exhibited the highest $\log_2$FC in response to MG in the B11221 background, independently of *MRR1a* (Table S1). We also observed, in all three *C. auris* strains, induction of several *MET* genes, which are involved in methionine synthesis and are an important branch of sulfur assimilation in yeast. Other genes involved in sulfur acquisition and assimilation that were induced by MG include the sulfate importer *SUL2*, a gene orthologous to both *CYS3* and *STR3* of *S. cerevisiae*, and numerous genes associated with iron-sulfur cluster formation (Table S1). A gene orthologous to *MUP1* of *S. cerevisiae* and *C. albicans* was induced by MG in B11221 WT and AR0390 but fell short of the $\log_2\text{FC} \geq 1.00$ cutoff in *mrr1a*Δ (Table S1 and Data Set S1). Induction of genes involved in sulfur metabolism, including the *MET* pathway, *SUL2*, *CYS3*, *STR3*, and *MUP1*, has previously been observed in *Saccharomyces cerevisiae* exposed to 1g/L acetaldehyde (113), another reactive aldehyde metabolite that is structurally similar to MG. Thus, sulfur acquisition and metabolism may be an important part of the carbonyl stress response in yeast.

In the B11221 background, we observed modest overlap in the genes and groups of genes that were up- or downregulated in response to either MG or BEN. *MDR1* and *MGD1* were among the genes induced by both compounds, and induction of *MGD1* by either MG or BEN was completely dependent on *MRR1a*. Although BEN, which originated as an agricultural fungicide, is widely recognized as an inducer of expression of Mrr1-regulated genes in *Candida* species (37, 41, 43, 95, 99–104), the mechanism by which this induction occurs is not yet known. BEN is thought to cause oxidative stress in yeast (114, 115), which is consistent with our observation of an upregulation of genes with a predicted role in oxidative stress response in BEN-treated *C. auris* cultures (Table S1). Additionally, in mammalian cells, BEN exposure has been shown to inhibit aldehyde dehydrogenase enzymes (116–119), which may lead to an accumulation of reactive aldehydes, although this possible mechanism has not yet been investigated in fungi.

We also note similarities between the results of our study of MG- and BEN-treated *C. auris* and the recently published transcriptional analysis of the clade I *C. auris* strain NCPF 8973 exposed to 75 μM farnesol (120). In response to farnesol, the authors reported upregulation of many genes with predicted roles in transmembrane

transport, such as *MDR1* and *CDR1*, and downregulation of numerous genes predicted to be involved in metal acquisition and homeostasis, including multiple ferric reductases and iron permeases (120). As farnesol may cause oxidative stress in *Candida* species (120–123) and in *S. cerevisiae* (124, 125), the overlap in transcriptional changes in response to MG, BEN, and farnesol likely provides valuable insight into how *C. auris* and other *Candida* species sense and adapt to physiologically relevant stressors. In fact, MG itself may serve as a stress signal in various organisms. In plants, for example, intracellular MG increases in response to drought (126, 127), salinity (126, 128–131), cold stress (126), heavy metals (128), or phosphorous deficiency (131), and overexpression of certain genes involved in MG detoxification has been shown to enhance salt tolerance in tobacco (126) and in *Brassica juncea* (132). Investigating whether MG detoxification is linked to abiotic stressors such as salt, temperature, or desiccation in *Candida* species would be an interesting avenue of future research, particularly in *C. auris* due to its persistence on hospital surfaces and high salt tolerance.

MATERIALS AND METHODS

Strains, media, and growth conditions. The sources of all strains used in this study are listed in Table S4. All strains were stored long term in a final concentration of 25% glycerol at −80°C and freshly streaked onto YPD agar (10 g/L yeast extract, 20 g/L peptone, 2% glucose, 1.5% agar) once every 7 days and maintained at room temperature. Unless otherwise noted, all overnight cultures were grown in 5 mL YPD liquid medium (10 g/L yeast extract, 20 g/L peptone, 2% glucose) on a rotary wheel at 30°C. Media was supplemented with 25 μg/mL BEN (stock 10 mg/mL in DMSO) or 5 mM, 10 mM, or 15 mM MG (Sigma-Aldrich, 5.55 M) as noted. *Escherichia coli* strains were grown in LB with 15 μg/mL gentamicin (gent).

Plasmids for complementation of *C. auris MRR1a*. Plasmids for complementing *C. auris MRR1a* into *C. lusitaniae* were created as follows: the open reading frame of *MRR1a* was amplified from the genomic DNA of *C. auris* isolates B11221 (for *CauMRR1a*^{N647T}) and AR0390 (for *CauMRR1a*) using a forward primer with homology to the 5′ flank of *C. lusitaniae MRR1* and a reverse primer with homology to the 3′ flank of *C. lusitaniae MRR1* for recombination into the *C. lusitaniae MRR1* complementation plasmid pMQ30$^{MRR1\text{-}L1191H+Q1197*}$ (58). Plasmid *pMQ30*$^{MRR1\text{-}L1191H+Q1197*}$ was digested with AscI (New England BioLabs) and AgeI-HF (New England BioLabs). The PCR products and digested plasmid were cleaned using the Zymo DNA Clean & Concentrator kit (Zymo Research) and assembled using the *S. cerevisiae* recombination technique described in (133). Recombined plasmids were isolated from *S. cerevisiae* using a yeast plasmid miniprep kit (Zymo Research) before transformation into NEB®5-alpha competent *E. coli* (New England BioLabs). *E. coli* containing pMQ30-derived plasmids were selected for on LB containing 15 μg/mL gentamicin. Plasmids from *E. coli* were isolated using a Zyppy Plasmid Miniprep kit (Zymo Research) and subsequently verified by Sanger sequencing with the Dartmouth College Genomics and Molecular Biology Shared Resources Core. *MRR1a* complementation plasmids containing the correct sequences were linearized with NotI-HF (New England BioLabs), cleaned up with the Zymo DNA Clean & Concentrator kit (Zymo Research) and eluted in molecular biology grade water (Corning) before transformation of 1.5 μg into *C. lusitaniae* strain U04 *mrr1*Δ as described below. All plasmids and primers used and created in this study are listed in Table S4.

Transformation of *C. lusitaniae* with *C. auris MRR1a* complementation constructs. Mutants in *C. lusitaniae* were generated using an expression-free CRISPR-Cas9 method as previously described (37, 58, 134). In brief, cells suspended in 1M sorbitol were electroporated immediately following the addition of 1.5 μg of *C. auris MRR1a* complementation plasmid that had been previously linearized with NotI-HF (New England BioLabs) and Cas9 ribonucleoprotein containing crRNA targeting the *NAT1* gene. Transformants were selected on YPD agar containing 600 μg/mL hygromycin B (HygB). Successful transformants were identified via PCR of the *C. lusitaniae MRR1* locus as previously described (37, 58). CRISPR RNAs (crRNAs; IDT) and primers used to validate transformants are listed in Table S4.

MIC assay. MIC assays for FLZ were performed in RPMI 1640 medium (Sigma, containing L-glutamine, 165 mM MOPS, 2% glucose at pH 7) as described in Demers et al. (40) and Biermann et al. (58) using the broth microdilution method. The final concentration of FLZ in each well ranged from 64 μg/mL to 0.125 μg/mL. Plates were incubated at 35°C and scored for growth at 24 h and 48 h; the results are reported in Table S4. The MIC was defined as the drug concentration that abolished visible growth compared with a drug-free control.

Growth kinetics. Growth kinetic assays were performed as previously described in Biermann et al. (58). In brief, exponential-phase cultures of *C. auris* or *C. lusitaniae* were washed and diluted in dH_2O to an OD_{600} of 1; 60 μL of each diluted cell suspension was added to 5 mL fresh YPD. To each well of a clear 96-well flat-bottom plate (Falcon) was added 100 μL of YPD or YPD with MG at twice the desired final concentration and 100 μL of cell inoculum in YPD. Plates were arranged in technical triplicate for each strain and condition and incubated in a Synergy Neo2 Microplate Reader (BioTek, USA) according to the following protocol: heat to 37°C, start kinetic, read OD_{600} every 60 min for 36 h, end kinetic. Results were calculated in Microsoft Excel and plotted in GraphPad Prism 9.0.0 (GraphPad Software).

Quantitative real-time PCR. Overnight cultures of *C. auris* or *C. lusitaniae* were diluted 1:50 into 5 mL fresh YPD, and grown to for 4 h at 37°C. To each culture was added MG to a final concentration of 5 mM (4.5 μL stock), BEN to a final concentration of 25 μg/mL (12.5 μL stock), or 4.5 μL molecular

biology grade dH_2O. Cultures were returned to the roller drum at 37°C for 15 min (MG or dH_2O) or 30 min (BEN), then centrifuged at 5,000 rpm for 5 min. The differences in time of exposure in the experimental scheme was used to maintain consistency with published experiments in other species, and not because of known differences in kinetics of activity for the two inducers. RNA isolation, gDNA removal, cDNA synthesis, and quantitative real-time PCR were performed as previously described (40). Transcripts were normalized to *C. auris* or *C. lusitaniae ACT1* expression as appropriate. Results were calculated in Microsoft Excel and plotted in GraphPad Prism 9.0.0 (GraphPad Software). Primers are listed in Table S4.

RNA sequencing. Overnight cultures of *C. auris* were diluted to an OD_{600} of 0.1 in 5 mL fresh, pre-warmed YPD, and incubated on a roller drum at 37°C for five to six doublings (approximately 6 h). Cultures were diluted once more to an OD_{600} of 1 in 5 mL fresh, pre-warmed YPD and returned to the roller drum at 37°C for another five to six doublings. To each culture was added MG to a final concentration of 5 mM (4.5 μL), BEN to a final concentration of 25 μg/mL (12.5 μL), or 4.5 μL molecular biology grade dH_2O. Cultures were returned to the roller drum at 37°C for 15 min (MG or dH_2O) or 30 min (BEN), then centrifuged at 5,000 rpm for 5 min. Supernatants were discarded and RNA isolation was performed on cell pellets as described above for qRT-PCR. gDNA was removed from RNA samples as described above. DNA-free RNA samples were sent to the Microbial Genome Sequencing Center (https://www.migscenter.com/) for RNA sequencing.

Analysis of RNA-seq. RNA-seq data were analyzed by the Microbial Genome Sequencing Center (https://www.migscenter.com/) as follows: Quality control and adapter trimming was performed with bcl2fastq (https://support.illumina.com/sequencing/sequencing_software/bcl2fastq-conversion-software.html). Read mapping was performed with HISAT2 (135). Read quantification was performed using Subread's featureCounts (136) functionality. Read counts were loaded into R (https://www.R-project.org/) and normalized using edgeR's (137) Trimmed Mean of M values (TMM) algorithm. Subsequent values were then converted to counts per million (cpm). Differential expression analysis was performed using edgeR's Quasi Linear F-Test. In the supplementary file, the sheet named "All Quantified Genes" contain the results of the exact test for all genes in addition to the normalized counts per million for all samples. Differentially expressed genes were determined using the cutoff of $|\log_2 FC| > 1$ and $P < 0.05$.

Identification of orthologs. Orthologs of *C. auris* genes in *C. albicans*, *C. lusitaniae*, and *S. cerevisiae*, as well as orthologs between B11221 and the clade I reference strain B8441, were identified using FungiDB (https://fungidb.org) (138, 139).

Generation of Venn diagrams. Venn diagrams of differentially expressed genes across different strains and conditions were computed using the Venn diagram tool from UGent Bioinformatics & Evolutionary Genomics, which is accessible at https://bioinformatics.psb.ugent.be/webtools/Venn/.

Statistical analysis and figure preparation. All graphs were prepared with GraphPad Prism 9.0.0 (GraphPad Software). Ratio paired t-tests and one-way ANOVA tests were performed in Prism; details on each test are described in the corresponding figure legends. All *P*-values were two-tailed and $P < 0.05$ were considered significant for all analyses performed and are indicated with asterisks in the text: * $p < 0.05$; ** $p < 0.01$; *** $p < 0.001$; **** $p < 0.0001$.

Data availability. The data supporting the findings in this study are available within the paper and its supplemental material and are also available from the corresponding author upon request. The raw sequence reads from the RNA-seq analysis have been deposited into NCBI sequence read archive under BioProject PRJNA801628 (https://www.ncbi.nlm.nih.gov/bioproject/PRJNA801628).

SUPPLEMENTAL MATERIAL

Supplemental material is available online only.

DATA SET S1, XLSX file, 5.6 MB.
FIG S1, TIF file, 0.3 MB.
FIG S2, TIF file, 0.3 MB.
FIG S3, TIF file, 0.2 MB.
FIG S4, TIF file, 0.2 MB.
FIG S5, TIF file, 0.2 MB.
TABLE S1, DOCX file, 0.1 MB.
TABLE S2, DOCX file, 0.02 MB.
TABLE S3, DOCX file, 0.04 MB.
TABLE S4, DOCX file, 0.04 MB.

ACKNOWLEDGMENTS

We thank Joachim Morschhäuser and the FDA-CDC Antimicrobial Resistance Isolate Bank for providing strains. We thank Judith Berman for the pGEM-*URA3* plasmid used for yeast cloning. We thank Elora Demers for primers.

A.R.B. and D.A.H. conceived and designed the experiments and wrote the paper; A.R.B. performed the experiments; A.R.B. and D.A.H. analyzed the data.

This study was supported by grants R01 5R01 AI127548 to D.A.H. Core services were provided by STANTO19R0 to CFF RDP, P30-DK117469 to DartCF, and P20-GM113132 to

BioMT. Sequencing services and specialized equipment were provided by the Genomics and Molecular Biology Shared Resource Core at Dartmouth, NCI Cancer Center Support Grant 5P30 CA023108-41. The content is solely the responsibility of the authors and does not necessarily represent the official views of the NIH.

The authors have declared that no competing interests exist.

REFERENCES

1. Pfaller MA, Andes DR, Diekema DJ, Horn DL, Reboli AC, Rotstein C, Franks B, Azie NE. 2014. Epidemiology and outcomes of invasive candidiasis due to non-albicans species of *Candida* in 2,496 patients: data from the Prospective Antifungal Therapy (PATH) registry 2004–2008. PLoS One 9:e101510. https://doi.org/10.1371/journal.pone.0101510.
2. Pfaller MA, Diekema DJ. 2007. Epidemiology of invasive candidiasis: a persistent public health problem. Clin Microbiol Rev 20:133–163. https://doi.org/10.1128/CMR.00029-06.
3. Quindos G, Marcos-Arias C, San-Millan R, Mateo E, Eraso E. 2018. The continuous changes in the aetiology and epidemiology of invasive candidiasis: from familiar *Candida albicans* to multiresistant *Candida auris*. Int Microbiol 21:107–119. https://doi.org/10.1007/s10123-018-0014-1.
4. Abe M, Kinjo Y, Ueno K, Takatsuka S, Nakamura S, Ogura S, Kimura M, Araoka H, Sadamoto S, Shinozaki M, Shibuya K, Yoneyama A, Kaku M, Miyazaki Y. 2018. Differences in ocular complications between *Candida albicans* and non-albicans *Candida* infection analyzed by epidemiology and a mouse ocular candidiasis model. Front Microbiol 9:2477. https://doi.org/10.3389/fmicb.2018.02477.
5. Leeyaphan C, Bunyaratavej S, Foongladda S, Rujitharanawong C, Maneeprasopchoke P, Surawan T, Muanprasat C, Matthapan L. 2016. Epidemiology, clinical characteristics, sites of infection and treatment outcomes of mucocutaneous Candidiasis caused by non-albicans species of *Candida* at a dermatologic clinic. J Med Assoc Thai 99:406–411.
6. Quindos G. 2014. Epidemiology of candidaemia and invasive candidiasis. a changing face. Rev Iberoam Micol 31:42–48. https://doi.org/10.1016/j.riam.2013.10.001.
7. Patel PK, Erlandsen JE, Kirkpatrick WR, Berg DK, Westbrook SD, Louden C, Cornell JE, Thompson GR, Vallor AC, Wickes BL, Wiederhold NP, Redding SW, Patterson TF. 2012. The changing epidemiology of oropharyngeal candidiasis in patients with HIV/AIDS in the era of antiretroviral therapy. AIDS Res Treat 2012:262471. https://doi.org/10.1155/2012/262471.
8. Hachem R, Hanna H, Kontoyiannis D, Jiang Y, Raad I. 2008. The changing epidemiology of invasive candidiasis: *Candida glabrata* and *Candida krusei* as the leading causes of candidemia in hematologic malignancy. Cancer 112:2493–2499. https://doi.org/10.1002/cncr.23466.
9. Redding SW, Kirkpatrick WR, Dib O, Fothergill AW, Rinaldi MG, Patterson TF. 2000. The epidemiology of non-albicans *Candida* in oropharyngeal candidiasis in HIV patients. Spec Care Dentist 20:178–181. https://doi.org/10.1111/j.1754-4505.2000.tb00015.x.
10. Abi-Said D, Anaissie E, Uzun O, Raad I, Pinzcowski H, Vartivarian S. 1997. The epidemiology of hematogenous candidiasis caused by different *Candida* species. Clin Infect Dis 24:1122–1128. https://doi.org/10.1086/513663.
11. Bravo Ruiz G, Lorenz A. 2021. What do we know about the biology of the emerging fungal pathogen of humans *Candida auris*? Microbiol Res 242:126621. https://doi.org/10.1016/j.micres.2020.126621.
12. Du H, Bing J, Hu T, Ennis CL, Nobile CJ, Huang G. 2020. *Candida auris*: epidemiology, biology, antifungal resistance, and virulence. PLoS Pathog 16:e1008921. https://doi.org/10.1371/journal.ppat.1008921.
13. Satoh K, Makimura K, Hasumi Y, Nishiyama Y, Uchida K, Yamaguchi H. 2009. *Candida auris* sp. nov., a novel ascomycetous yeast isolated from the external ear canal of an inpatient in a Japanese hospital. Microbiol Immunol 53:41–44. https://doi.org/10.1111/j.1348-0421.2008.00083.x.
14. Lee WG, Shin JH, Uh Y, Kang MG, Kim SH, Park KH, Jang HC. 2011. First three reported cases of nosocomial fungemia caused by *Candida auris*. J Clin Microbiol 49:3139–3142. https://doi.org/10.1128/JCM.00319-11.
15. Lockhart SR, Etienne KA, Vallabhaneni S, Farooqi J, Chowdhary A, Govender NP, Colombo AL, Calvo B, Cuomo CA, Desjardins CA, Berkow EL, Castanheira M, Magobo RE, Jabeen K, Asghar RJ, Meis JF, Jackson B, Chiller T, Litvintseva AP. 2017. Simultaneous emergence of multidrug-resistant *Candida auris* on 3 continents confirmed by whole-genome sequencing and epidemiological analyses. Clin Infect Dis 64:134–140. https://doi.org/10.1093/cid/ciw691.
16. Chow NA, de Groot T, Badali H, Abastabar M, Chiller TM, Meis JF. 2019. Potential fifth clade of *Candida auris*, Iran, 2018. Emerg Infect Dis 25:1780–1781. https://doi.org/10.3201/eid2509.190686.
17. Proctor DM, Dangana T, Sexton DJ, Fukuda C, Yelin RD, Stanley M, Bell PB, Baskaran S, Deming C, Chen Q, Conlan S, Park M, Mullikin J, Thomas J, Young A, Bouffard G, Barnabas B, Brooks S, Han J, Ho S-I, Kim J, Legaspi R, Maduro Q, Marfani H, Montemayor C, Riebow N, Schandler K, Schmidt B, Sison C, Stantripop M, Black S, Dekhtyar M, Masiello C, McDowell J, Thomas P, Vemulapalli M, Welsh RM, Vallabhaneni S, Chiller T, Forsberg K, Black SR, Pacilli M, Kong HH, Lin MY, Schoeny ME, Litvintseva AP, Segre JA, Hayden MK, NISC Comparative Sequencing Program. 2021. Integrated genomic, epidemiologic investigation of *Candida auris* skin colonization in a skilled nursing facility. Nat Med 27:1401–1409. https://doi.org/10.1038/s41591-021-01383-w.
18. Horton MV, Johnson CJ, Kernien JF, Patel TD, Lam BC, Cheong JZA, Meudt JJ, Shanmuganayagam D, Kalan LR, Nett JE. 2020. *Candida auris* forms high-burden biofilms in skin niche conditions and on porcine skin. mSphere 5. https://doi.org/10.1128/mSphere.00910-19.
19. Uppuluri P. 2020. Candida auris biofilm colonization on skin niche conditions. mSphere 5. https://doi.org/10.1128/mSphere.00972-19.
20. Osei Sekyere J. 2018. *Candida auris*: A systematic review and meta-analysis of current updates on an emerging multidrug-resistant pathogen. Microbiologyopen 7:e00578. https://doi.org/10.1002/mbo3.578.
21. Taori SK, Khonyongwa K, Hayden I, Athukorala GDA, Letters A, Fife A, Desai N, Borman AM. 2019. *Candida auris* outbreak: mortality, interventions and cost of sustaining control. J Infect 79:601–611. https://doi.org/10.1016/j.jinf.2019.09.007.
22. Arensman K, Miller JL, Chiang A, Mai N, Levato J, LaChance E, Anderson M, Beganovic M, Dela Pena J. 2020. Clinical outcomes of patients treated for *Candida auris* infections in a multisite health system, Illinois, USA. Emerg Infect Dis 26:876–880. https://doi.org/10.3201/eid2605.191588.
23. AlJindan R, AlEraky DM, Mahmoud N, Abdalhamid B, Almustafa M, AbdulAzeez S, Borgio JF. 2020. Drug resistance-associated mutations in *ERG11* of multidrug-resistant *Candida auris* in a tertiary care hospital of Eastern Saudi Arabia. J Fungi (Basel) 7.
24. Carolus H, Pierson S, Munoz JF, Subotic A, Cruz RB, Cuomo CA, Van Dijck P. 2021. Genome-wide analysis of experimentally evolved *Candida auris* reveals multiple novel mechanisms of multidrug resistance. mBio 12. https://doi.org/10.1128/mBio.03333-20.
25. Chow NA, Munoz JF, Gade L, Berkow EL, Li X, Welsh RM, Forsberg K, Lockhart SR, Adam R, Alanio A, Alastruey-Izquierdo A, Althawadi S, Arauz AB, Ben-Ami R, Bharat A, Calvo B, Desnos-Ollivier M, Escandon P, Gardam D, Gunturu R, Heath CH, Kurzai O, Martin R, Litvintseva AP, Cuomo CA. 2020. Tracing the evolutionary history and global expansion of *Candida auris* using population genomic analyses. mBio 11. https://doi.org/10.1128/mBio.03364-19.
26. Chowdhary A, Prakash A, Sharma C, Kordalewska M, Kumar A, Sarma S, Tarai B, Singh A, Upadhyaya G, Upadhyay S, Yadav P, Singh PK, Khillan V, Sachdeva N, Perlin DS, Meis JF. 2018. A multicentre study of antifungal susceptibility patterns among 350 *Candida auris* isolates (2009–17) in India: role of the *ERG11* and *FKS1* genes in azole and echinocandin resistance. J Antimicrob Chemother 73:891–899. https://doi.org/10.1093/jac/dkx480.
27. Healey KR, Kordalewska M, Jimenez Ortigosa C, Singh A, Berrio I, Chowdhary A, Perlin DS. 2018. Limited *ERG11* mutations identified in isolates of *Candida auris* directly contribute to reduced azole susceptibility. Antimicrob Agents Chemother 62. https://doi.org/10.1128/AAC.01427-18.
28. Li J, Coste AT, Liechti M, Bachmann D, Sanglard D, Lamoth F. 2021. Novel *ERG11* and *TAC1b* mutations associated with azole resistance in *Candida auris*. Antimicrob Agents Chemother.
29. Munoz JF, Gade L, Chow NA, Loparev VN, Juieng P, Berkow EL, Farrer RA, Litvintseva AP, Cuomo CA. 2018. Genomic insights into multidrug-

resistance, mating and virulence in *Candida auris* and related emerging species. Nat Commun 9:5346. https://doi.org/10.1038/s41467-018-07779-6.
30. Rybak JM, Sharma C, Doorley LA, Barker KS, Palmer GE, Rogers PD. 2021. Delineation of the direct contribution of *Candida auris ERG11* mutations to clinical triazole resistance. Microbiol Spectr 9:e0158521. https://doi.org/10.1128/Spectrum.01585-21.
31. Williamson B, Wilk A, Guerrero KD, Mikulski TD, Elias TN, Sawh I, Cancino-Prado G, Gardam D, Heath CH, Govender NP, Perlin DS, Kordalewska M, Healey KR. 2022. Impact of Erg11 amino acid substitutions identified in *Candida auris* Clade III isolates on triazole drug susceptibility. Antimicrob Agents Chemother 66:e0162421. https://doi.org/10.1128/AAC.01624-21.
32. Rybak JM, Doorley LA, Nishimoto AT, Barker KS, Palmer GE, Rogers PD. 2019. Abrogation of triazole resistance upon deletion of *CDR1* in a clinical isolate of *Candida auris*. Antimicrob Agents Chemother 63. https://doi.org/10.1128/AAC.00057-19.
33. Kim SH, Iyer KR, Pardeshi L, Munoz JF, Robbins N, Cuomo CA, Wong KH, Cowen LE. 2019. Genetic analysis of *Candida auris* implicates Hsp90 in morphogenesis and azole tolerance and Cdr1 in azole resistance. mBio 10.
34. Kim SH, Iyer KR, Pardeshi L, Munoz JF, Robbins N, Cuomo CA, Wong KH, Cowen LE. 2019. Erratum for Kim et al., Genetic analysis of *Candida auris* implicates Hsp90 in morphogenesis and azole tolerance and Cdr1 in azole resistance. mBio 10.
35. Rybak JM, Munoz JF, Barker KS, Parker JE, Esquivel BD, Berkow EL, Lockhart SR, Gade L, Palmer GE, White TC, Kelly SL, Cuomo CA, Rogers PD. 2020. Mutations in *TAC1B*: a novel genetic determinant of clinical fluconazole resistance in *Candida auris*. mBio 11. https://doi.org/10.1128/mBio.00365-20.
36. Wasi M, Khandelwal NK, Moorhouse AJ, Nair R, Vishwakarma P, Bravo Ruiz G, Ross ZK, Lorenz A, Rudramurthy SM, Chakrabarti A, Lynn AM, Mondal AK, Gow NAR, Prasad R. 2019. ABC transporter genes show upregulated expression in drug-resistant clinical isolates of *Candida auris*: a genome-wide characterization of ATP-binding cassette (ABC) transporter genes. Front Microbiol 10:1445. https://doi.org/10.3389/fmicb.2019.01445.
37. Demers EG, Stajich JE, Ashare A, Occhipinti P, Hogan DA. 2021. Balancing positive and negative selection: *in vivo* evolution of *Candida lusitaniae MRR1*. mBio 12. https://doi.org/10.1128/mBio.03328-20.
38. Liu Z, Myers LC. 2017. *Candida albicans* Swi/Snf and Mediator complexes differentially regulate Mrr1-induced *MDR1* expression and fluconazole resistance. Antimicrob Agents Chemother 61. https://doi.org/10.1128/AAC.01344-17.
39. Kannan A, Asner SA, Trachsel E, Kelly S, Parker J, Sanglard D. 2019. Comparative genomics for the elucidation of multidrug resistance in *Candida lusitaniae*. mBio 10. https://doi.org/10.1128/mBio.02512-19.
40. Demers EG, Biermann AR, Masonjones S, Crocker AW, Ashare A, Stajich JE, Hogan DA. 2018. Evolution of drug resistance in an antifungal-naive chronic *Candida lusitaniae* infection. Proc Natl Acad Sci U S A 115:12040–12045. https://doi.org/10.1073/pnas.1807698115.
41. Schubert S, Popp C, Rogers PD, Morschhauser J. 2011. Functional dissection of a *Candida albicans* zinc cluster transcription factor, the multidrug resistance regulator Mrr1. Eukaryot Cell 10:1110–1121. https://doi.org/10.1128/EC.05100-11.
42. Schubert S, Rogers PD, Morschhauser J. 2008. Gain-of-function mutations in the transcription factor *MRR1* are responsible for overexpression of the *MDR1* efflux pump in fluconazole-resistant *Candida dubliniensis* strains. Antimicrob Agents Chemother 52:4274–4280. https://doi.org/10.1128/AAC.00740-08.
43. Schneider S, Morschhauser J. 2015. Induction of *Candida albicans* drug resistance genes by hybrid zinc cluster transcription factors. Antimicrob Agents Chemother 59:558–569. https://doi.org/10.1128/AAC.04448-14.
44. Schubert S, Barker KS, Znaidi S, Schneider S, Dierolf F, Dunkel N, Aid M, Boucher G, Rogers PD, Raymond M, Morschhauser J. 2011. Regulation of efflux pump expression and drug resistance by the transcription factors Mrr1, Upc2, and Cap1 in *Candida albicans*. Antimicrob Agents Chemother 55:2212–2223. https://doi.org/10.1128/AAC.01343-10.
45. Morschhauser J, Barker KS, Liu TT, Bla BWJ, Homayouni R, Rogers PD. 2007. The transcription factor Mrr1p controls expression of the *MDR1* efflux pump and mediates multidrug resistance in *Candida albicans*. PLoS Pathog 3:e164. https://doi.org/10.1371/journal.ppat.0030164.
46. Mayr EM, Ramirez-Zavala B, Kruger I, Morschhauser J. 2020. A zinc cluster transcription factor contributes to the intrinsic fluconazole resistance of *Candida auris*. mSphere 5. https://doi.org/10.1128/mSphere.00279-20.
47. Spivak ES, Hanson KE. 2018. *Candida auris*: an emerging fungal pathogen. J Clin Microbiol 56. https://doi.org/10.1128/JCM.01588-17.
48. Jin L, Cao Z, Wang Q, Wang Y, Wang X, Chen H, Wang H. 2018. *MDR1* overexpression combined with *ERG11* mutations induce high-level fluconazole resistance in *Candida tropicalis* clinical isolates. BMC Infect Dis 18:162. https://doi.org/10.1186/s12879-018-3082-0.
49. Liston SD, Whitesell L, Kapoor M, Shaw KJ, Cowen LE. 2020. Enhanced efflux pump expression in *Candida* mutants results in decreased manogepix susceptibility. Antimicrob Agents Chemother 64. https://doi.org/10.1128/AAC.00261-20.
50. Wirsching S, Moran GP, Sullivan DJ, Coleman DC, Morschhauser J. 2001. *MDR1*-mediated drug resistance in *Candida dubliniensis*. Antimicrob Agents Chemother 45:3416–3421. https://doi.org/10.1128/AAC.45.12.3416-3421.2001.
51. You L, Qian W, Yang Q, Mao L, Zhu L, Huang X, Jin J, Meng H. 2017. *ERG11* gene mutations and *MDR1* upregulation confer pan-azole resistance in *Candida tropicalis* causing disseminated candidiasis in an acute lymphoblastic leukemia patient on posaconazole prophylaxis. Antimicrob Agents Chemother 61. https://doi.org/10.1128/AAC.02496-16.
52. Wirsching S, Michel S, Morschhauser J. 2000. Targeted gene disruption in *Candida albicans* wild-type strains: the role of the *MDR1* gene in fluconazole resistance of clinical *Candida albicans* isolates. Mol Microbiol 36:856–865. https://doi.org/10.1046/j.1365-2958.2000.01899.x.
53. Berkow EL, Manigaba K, Parker JE, Barker KS, Kelly SL, Rogers PD. 2015. Multidrug transporters and alterations in sterol biosynthesis contribute to azole antifungal resistance in *Candida parapsilosis*. Antimicrob Agents Chemother 59:5942–5950. https://doi.org/10.1128/AAC.01358-15.
54. Souza AC, Fuchs BB, Pinhati HM, Siqueira RA, Hagen F, Meis JF, Mylonakis E, Colombo AL. 2015. *Candida parapsilosis* resistance to fluconazole: molecular mechanisms and *in vivo* impact in infected *Galleria mellonella* Larvae. Antimicrob Agents Chemother 59:6581–6587. https://doi.org/10.1128/AAC.01177-15.
55. Grossman NT, Pham CD, Cleveland AA, Lockhart SR. 2015. Molecular mechanisms of fluconazole resistance in *Candida parapsilosis* isolates from a U.S. surveillance system. Antimicrob Agents Chemother 59:1030–1037. https://doi.org/10.1128/AAC.04613-14.
56. Hampe IAI, Friedman J, Edgerton M, Morschhauser J. 2017. An acquired mechanism of antifungal drug resistance simultaneously enables *Candida albicans* to escape from intrinsic host defenses. PLoS Pathog 13:e1006655. https://doi.org/10.1371/journal.ppat.1006655.
57. Hiller D, Sanglard D, Morschhauser J. 2006. Overexpression of the *MDR1* gene is sufficient to confer increased resistance to toxic compounds in *Candida albicans*. Antimicrob Agents Chemother 50:1365–2591. https://doi.org/10.1128/AAC.50.4.1365-1371.2006.
58. Biermann AR, Demers EG, Hogan DA. 2021. Mrr1 regulation of methylglyoxal catabolism and methylglyoxal-induced fluconazole resistance in Candida lusitaniae. Mol Microbiol 115:116–130. https://doi.org/10.1111/mmi.14604.
59. Chakraborty S, Karmakar K, Chakravortty D. 2014. Cells producing their own nemesis: understanding methylglyoxal metabolism. Iubmb Life 66:667–678. https://doi.org/10.1002/iub.1324.
60. Tian S, Rong C, Nian H, Li F, Chu Y, Cheng S, Shang H. 2018. First cases and risk factors of super yeast *Candida auris* infection or colonization from Shenyang, China. Emerg Microbes Infect 7:128. https://doi.org/10.1038/s41426-018-0131-0.
61. Sayeed MA, Farooqi J, Jabeen K, Mahmood SF. 2020. Comparison of risk factors and outcomes of *Candida auris* candidemia with non-*Candida auris* candidemia: A retrospective study from Pakistan. Med Mycol 58:721–729. https://doi.org/10.1093/mmy/myz112.
62. Shastri PS, Shankarnarayan SA, Oberoi J, Rudramurthy SM, Wattal C, Chakrabarti A. 2020. *Candida auris* candidaemia in an intensive care unit - prospective observational study to evaluate epidemiology, risk factors, and outcome. J Crit Care 57:42–48. https://doi.org/10.1016/j.jcrc.2020.01.004.
63. Rudramurthy SM, Chakrabarti A, Paul RA, Sood P, Kaur H, Capoor MR, Kindo AJ, Marak RSK, Arora A, Sardana R, Das S, China D, Patel A, Xess I, Tarai B, Singh P, Ghosh A. 2017. *Candida auris* candidaemia in Indian ICUs: analysis of risk factors. J Antimicrob Chemother 72:1794–1801. https://doi.org/10.1093/jac/dkx034.
64. Ruiz-Gaitan A, Martinez H, Moret AM, Calabuig E, Tasias M, Alastruey-Izquierdo A, Zaragoza O, Mollar J, Frasquet J, Salavert-Lleti M, Ramirez P, Lopez-Hontangas JL, Peman J. 2019. Detection and treatment of *Candida auris* in an outbreak situation: risk factors for developing colonization and candidemia by this new species in critically ill patients. Expert Rev Anti Infect Ther 17:295–305. https://doi.org/10.1080/14787210.2019.1592675.

65. Al-Rashdi A, Al-Maani A, Al-Wahaibi A, Alqayoudhi A, Al-Jardani A, Al-Abri S. 2021. Characteristics, risk factors, and survival analysis of *Candida auris* cases: results of one-year national surveillance data from Oman. J Fungi (Basel) 7.
66. Caceres DH, Rivera SM, Armstrong PA, Escandon P, Chow NA, Ovalle MV, Diaz J, Derado G, Salcedo S, Berrio I, Espinosa-Bode A, Varon C, Stuckey MJ, Marino A, Villalobos N, Lockhart SR, Chiller TM, Prieto FE, Jackson BR. 2020. Case-case comparison of *Candida auris* versus other *Candida* species bloodstream infections: results of an outbreak investigation in Colombia. Mycopathologia 185:917–923. https://doi.org/10.1007/s11046-020-00478-1.
67. Khan Z, Ahmad S, Benwan K, Purohit P, Al-Obaid I, Bafna R, Emara M, Mokaddas E, Abdullah AA, Al-Obaid K, Joseph L. 2018. Invasive *Candida auris* infections in Kuwait hospitals: epidemiology, antifungal treatment and outcome. Infection 46:641–650. https://doi.org/10.1007/s15010-018-1164-y.
68. Pandya N, Cag Y, Pandak N, Pekok AU, Poojary A, Ayoade F, Fasciana T, Giammanco A, Caskurlu H, Rajani DP, Gupta YK, Balkan II, Khan EA, Erdem H. 2021. International Multicentre Study of *Candida auris* Infections. J Fungi (Basel) 7.
69. Rossow J, Ostrowsky B, Adams E, Greenko J, McDonald R, Vallabhaneni S, Forsberg K, Perez S, Lucas T, Alroy KA, Jacobs Slifka K, Walters M, Jackson BR, Quinn M, Chaturvedi S, Blog D, New York Candida auris Investigation Workgroup. 2021. Factors associated with *Candida auris* colonization and transmission in skilled nursing facilities with ventilator Units, New York, 2016–2018. Clin Infect Dis 72:e753–e760. https://doi.org/10.1093/cid/ciaa1462.
70. Wang XJ, Ma SB, Liu ZF, Li H, Gao WY. 2019. Elevated levels of alpha-dicarbonyl compounds in the plasma of type II diabetics and their relevance with diabetic nephropathy. J Chromatography B-Analytical Technologies in the Biomedical and Life Sciences 1106:19–25.
71. McLellan AC, Thornalley PJ, Benn J, Sonksen PH. 1994. Glyoxalase system in clinical diabetes mellitus and correlation with diabetic complications. Clin Sci (Lond) 87:21–29. https://doi.org/10.1042/cs0870021.
72. Lu J, Randell E, Han Y, Adeli K, Krahn J, Meng QH. 2011. Increased plasma methylglyoxal level, inflammation, and vascular endothelial dysfunction in diabetic nephropathy. Clin Biochem 44:307–311. https://doi.org/10.1016/j.clinbiochem.2010.11.004.
73. Odani H, Shinzato T, Usami J, Matsumoto Y, Brinkmann Frye E, Baynes JW, Maeda K. 1998. Imidazolium crosslinks derived from reaction of lysine with glyoxal and methylglyoxal are increased in serum proteins of uremic patients: evidence for increased oxidative stress in uremia. FEBS Lett 427:381–385. https://doi.org/10.1016/S0014-5793(98)00416-5.
74. Karg E, Papp F, Tassi N, Janaky T, Wittmann G, Turi S. 2009. Enhanced methylglyoxal formation in the erythrocytes of hemodialyzed patients. Metabolism 58:976–982. https://doi.org/10.1016/j.metabol.2009.02.032.
75. Lapolla A, Flamini R, Lupo A, Arico NC, Rugiu C, Reitano R, Tubaro M, Ragazzi E, Seraglia R, Traldi P. 2005. Evaluation of glyoxal and methylglyoxal levels in uremic patients under peritoneal dialysis. Ann N Y Acad Sci 1043:217–224. https://doi.org/10.1196/annals.1333.027.
76. Mukhopadhyay S, Ghosh A, Kar M. 2008. Methylglyoxal increase in uremia with special reference to snakebite-mediated acute renal failure. Clin Chim Acta 391:13–17. https://doi.org/10.1016/j.cca.2008.01.013.
77. Brenner T, Fleming T, Uhle F, Silaff S, Schmitt F, Salgado E, Ulrich A, Zimmermann S, Bruckner T, Martin E, Bierhaus A, Nawroth PP, Weigand MA, Hofer S. 2014. Methylglyoxal as a new biomarker in patients with septic shock: an observational clinical study. Crit Care 18. https://doi.org/10.1186/s13054-014-0683-x.
78. Juarez P, Jeannot K, Plesiat P, Llanes C. 2017. Toxic electrophiles induce expression of the multidrug efflux pump MexEF-OprN in *Pseudomonas aeruginosa* through a novel transcriptional regulator, CmrA. Antimicrob Agents Chemother 61. https://doi.org/10.1128/AAC.00585-17.
79. Ozyamak E, de Almeida C, de Moura AP, Miller S, Booth IR. 2013. Integrated stress response of *Escherichia coli* to methylglyoxal: transcriptional readthrough from the nemRA operon enhances protection through increased expression of glyoxalase I. Mol Microbiol 88:936–950. https://doi.org/10.1111/mmi.12234.
80. Lee C, Shin J, Park C. 2013. Novel regulatory system nemRA-gloA for electrophile reduction in *Escherichia coli* K-12. Mol Microbiol 88:395–412. https://doi.org/10.1111/mmi.12192.
81. Mostofa MG, Ghosh A, Li ZG, Siddiqui MN, Fujita M, Tran LP. 2018. Methylglyoxal - a signaling molecule in plant abiotic stress responses. Free Radic Biol Med 122:96–109. https://doi.org/10.1016/j.freeradbiomed.2018.03.009.
82. Kosmachevskaya OV, Shumaev KB, Topunov AF. 2017. Signal and regulatory effects of methylglyoxal in eukaryotic cells (review). Appl Biochem Microbiol 53:273–289. https://doi.org/10.1134/S0003683817030103.
83. Maeta K, Izawa S, Okazaki S, Kuge S, Inoue Y. 2004. Activity of the Yap1 transcription factor in *Saccharomyces cerevisiae* is modulated by methylglyoxal, a metabolite derived from glycolysis. Mol Cell Biol 24:8753–8764. https://doi.org/10.1128/MCB.24.19.8753-8764.2004.
84. Aguilera J, Prieto JA. 2004. Yeast cells display a regulatory mechanism in response to methylglyoxal. FEMS Yeast Res 4:633–641. https://doi.org/10.1016/j.femsyr.2003.12.007.
85. Roy A, Hashmi S, Li Z, Dement AD, Cho KH, Kim JH. 2016. The glucose metabolite methylglyoxal inhibits expression of the glucose transporter genes by inactivating the cell surface glucose sensors Rgt2 and Snf3 in yeast. Mol Biol Cell 27:862–871. https://doi.org/10.1091/mbc.E15-11-0789.
86. Anonymous. 2016. Correction for The glucose metabolite methylglyoxal inhibits expression of the glucose transporter genes by inactivating the cell surface glucose sensors Rgt2 and Snf3 in yeast. Mol Biol Cell 27:3178–3179. https://doi.org/10.1091/mboc.27.20.3178.
87. Maeta K, Izawa S, Inoue Y. 2005. Methylglyoxal, a metabolite derived from glycolysis, functions as a signal initiator of the high osmolarity glycerol-mitogen-activated protein kinase cascade and Calcineurin/Crz1-mediated pathway in *Saccharomyces cerevisiae*. J Biological Chemistry 280:253–260. https://doi.org/10.1074/jbc.M408061200.
88. Takatsume Y, Izawa S, Inoue Y. 2007. Modulation of Spc1 stress-activated protein kinase activity by methylglyoxal through inhibition of protein phosphatase in the fission yeast *Schizosaccharomyces pombe*. Biochem Biophys Res Commun 363:942–947. https://doi.org/10.1016/j.bbrc.2007.09.071.
89. Takatsume Y, Izawa S, Inoue Y. 2006. Methylglyoxal as a signal initiator for activation of the stress-activated protein kinase cascade in the fission yeast *Schizosaccharomyces pombe*. J Biol Chem 281:9086–9092. https://doi.org/10.1074/jbc.M511037200.
90. Welsh RM, Bentz ML, Shams A, Houston H, Lyons A, Rose LJ, Litvintseva AP. 2017. Survival, persistence, and isolation of the emerging multidrug-resistant pathogenic yeast *Candida auris* on a plastic health care surface. J Clin Microbiol 55:2996–3005. https://doi.org/10.1128/JCM.00921-17.
91. Rutala WA, Kanamori H, Gergen MF, Sickbert-Bennett EE, Weber DJ. 2019. Susceptibility of *Candida auris* and *Candida albicans* to 21 germicides used in healthcare facilities. Infect Control Hosp Epidemiol 40:380–382. https://doi.org/10.1017/ice.2019.1.
92. Jabeen K, Mal PB, Tharwani A, Hashmi M, Farooqi J. 2020. Persistence of *Candida auris* on latex and nitrile gloves with transmission to sterile urinary catheters double dagger. Med Mycol 58:128–132. https://doi.org/10.1093/mmy/myz033.
93. Eyre DW, Sheppard AE, Madder H, Moir I, Moroney R, Quan TP, Griffiths D, George S, Butcher L, Morgan M, Newnham R, Sunderland M, Clarke T, Foster D, Hoffman P, Borman AM, Johnson EM, Moore G, Brown CS, Walker AS, Peto TEA, Crook DW, Jeffery KJM. 2018. A *Candida auris* outbreak and its control in an intensive care setting. N Engl J Med 379:1322–1331. https://doi.org/10.1056/NEJMoa1714373.
94. Hoehamer CF, Cummings ED, Hilliard GM, Morschhauser J, Rogers PD. 2009. Proteomic analysis of Mrr1p- and Tac1p-associated differential protein expression in azole-resistant clinical isolates of *Candida albicans*. Proteomics Clin Appl 3:968–978. https://doi.org/10.1002/prca.200800252.
95. Karababa M, Coste AT, Rognon B, Bille J, Sanglard D. 2004. Comparison of gene expression profiles of *Candida albicans* azole-resistant clinical isolates and laboratory strains exposed to drugs inducing multidrug transporters. Antimicrob Agents Chemother 48:3064–3079. https://doi.org/10.1128/AAC.48.8.3064-3079.2004.
96. Rogers PD, Barker KS. 2003. Genome-wide expression profile analysis reveals coordinately regulated genes associated with stepwise acquisition of azole resistance in *Candida albicans* clinical isolates. Antimicrob Agents Chemother 47:1220–1227. https://doi.org/10.1128/AAC.47.4.1220-1227.2003.
97. Silva AP, Miranda IM, Guida A, Synnott J, Rocha R, Silva R, Amorim A, Pina-Vaz C, Butler G, Rodrigues AG. 2011. Transcriptional profiling of azole-resistant *Candida parapsilosis* strains. Antimicrob Agents Chemother 55:3546–3556. https://doi.org/10.1128/AAC.01127-10.
98. Kannan A, Asner SA, Trachsel E, Kelly S, Parker J, Sanglard D. 2020. Erratum for Kannan et al., Comparative genomics for the elucidation of multidrug resistance in *Candida lusitaniae*. mBio 11. https://doi.org/10.1128/mBio.03403-19.
99. Rognon B, Kozovska Z, Coste AT, Pardini G, Sanglard D. 2006. Identification of promoter elements responsible for the regulation of *MDR1* from

Candida albicans, a major facilitator transporter involved in azole resistance. Microbiology (Reading) 152:3701–3722. https://doi.org/10.1099/mic.0.29277-0.
100. Ramirez-Zavala B, Mogavero S, Scholler E, Sasse C, Rogers PD, Morschhauser J. 2014. SAGA/ADA complex subunit Ada2 is required for Cap1- but not Mrr1-mediated upregulation of the *Candida albicans* multidrug efflux pump *MDR1*. Antimicrob Agents Chemother 58:5102–5110. https://doi.org/10.1128/AAC.03065-14.
101. Mogavero S, Tavanti A, Senesi S, Rogers PD, Morschhauser J. 2011. Differential requirement of the transcription factor Mcm1 for activation of the *Candida albicans* multidrug efflux pump *MDR1* by its regulators Mrr1 and Cap1. Antimicrob Agents Chemother 55:2061–2066. https://doi.org/10.1128/AAC.01467-10.
102. Hiller D, Stahl S, MorschhäUser J. 2006. Multiple cis-acting sequences mediate upregulation of the *MDR1* efflux pump in a fluconazole-resistant clinical *Candida albicans* isolate. Antimicrob Agents Chemother 50:2300–2308. https://doi.org/10.1128/AAC.00196-06.
103. Harry JB, Oliver BG, Song JL, Silver PM, Little JT, Choiniere J, White TC. 2005. Drug-induced regulation of the *MDR1* promoter in *Candida albicans*. Antimicrob Agents Chemother 49:2785–2792. https://doi.org/10.1128/AAC.49.7.2785-2792.2005.
104. Gupta V, Kohli A, Krishnamurthy S, Puri N, Aalamgeer SA, Panwar S, Prasad R. 1998. Identification of polymorphic mutant alleles of *CaMDR1*, a major facilitator of *Candida albicans* which confers multidrug resistance, and its *in vitro* transcriptional activation. Curr Genet 34:192–199. https://doi.org/10.1007/s002940050385.
105. Iyer KR, Camara K, Daniel-Ivad M, Trilles R, Pimentel-Elardo SM, Fossen JL, Marchillo K, Liu Z, Singh S, Munoz JF, Kim SH, Porco JA, Jr, Cuomo CA, Williams NS, Ibrahim AS, Edwards JE, Jr, Andes DR, Nodwell JR, Brown LE, Whitesell L, Robbins N, Cowen LE. 2020. An oxindole efflux inhibitor potentiates azoles and impairs virulence in the fungal pathogen *Candida auris*. Nat Commun 11:6429. https://doi.org/10.1038/s41467-020-20183-3.
106. Dunkel N, Blass J, Rogers PD, Morschhauser J. 2008. Mutations in the multi-drug resistance regulator *MRR1*, followed by loss of heterozygosity, are the main cause of *MDR1* overexpression in fluconazole-resistant *Candida albicans* strains. Mol Microbiol 69:827–840. https://doi.org/10.1111/j.1365-2958.2008.06309.x.
107. Rodrigues CF, Rodrigues ME, Henriques M. 2019. *Candida* sp. infections in patients with diabetes mellitus. J Clin Med 8.
108. Pyrgos V, Ratanavanich K, Donegan N, Veis J, Walsh TJ, Shoham S. 2009. *Candida* bloodstream infections in hemodialysis recipients. Med Mycol 47:463–467. https://doi.org/10.1080/13693780802369332.
109. Zhang MM, Ong CL, Walker MJ, McEwan AG. 2016. Defence against methylglyoxal in group A *Streptococcus*: a role for Glyoxylase I in bacterial virulence and survival in neutrophils? Pathog Dis 74.
110. Rachman H, Kim N, Ulrichs T, Baumann S, Pradl L, Nasser Eddine A, Bild M, Rother M, Kuban RJ, Lee JS, Hurwitz R, Brinkmann V, Kosmiadi GA, Kaufmann SH. 2006. Critical role of methylglyoxal and AGE in mycobacteria-induced macrophage apoptosis and activation. PLoS One 1:e29. https://doi.org/10.1371/journal.pone.0000029.
111. Prantner D, Nallar S, Richard K, Spiegel D, Collins KD, Vogel SN. 2021. Classically activated mouse macrophages produce methylglyoxal that induces a TLR4- and RAGE-independent proinflammatory response. J Leukoc Biol 109:605–619. https://doi.org/10.1002/JLB.3A0520-745RR.
112. Jimenez-Lopez C, Collette JR, Brothers KM, Shepardson KM, Cramer RA, Wheeler RT, Lorenz MC. 2013. *Candida albicans* induces arginine biosynthetic genes in response to host-derived reactive oxygen species. Eukaryot Cell 12:91–100. https://doi.org/10.1128/EC.00290-12.
113. Aranda A, del Olmo ML. 2004. Exposure of *Saccharomyces cerevisiae* to acetaldehyde induces sulfur amino acid metabolism and polyamine transporter genes, which depend on Met4p and Haa1p transcription factors, respectively. Appl Environ Microbiol 70:1913–1922. https://doi.org/10.1128/AEM.70.4.1913-1922.2004.
114. Lucau-Danila A, Lelandais G, Kozovska Z, Tanty V, Delaveau T, Devaux F, Jacq C. 2005. Early expression of yeast genes affected by chemical stress. Mol Cell Biol 25:1860–1868. https://doi.org/10.1128/MCB.25.5.1860-1868.2005.
115. Lelandais G, Tanty V, Geneix C, Etchebest C, Jacq C, Devaux F. 2008. Genome adaptation to chemical stress: clues from comparative transcriptomics in *Saccharomyces cerevisiae* and *Candida glabrata*. Genome Biol 9:R164. https://doi.org/10.1186/gb-2008-9-11-r164.
116. Staub RE, Quistad GB, Casida JE. 1998. Mechanism for benomyl action as a mitochondrial aldehyde dehydrogenase inhibitor in mice. Chem Res Toxicol 11:535–543. https://doi.org/10.1021/tx980002l.
117. Fitzmaurice AG, Rhodes SL, Lulla A, Murphy NP, Lam HA, O'Donnell KC, Barnhill L, Casida JE, Cockburn M, Sagasti A, Stahl MC, Maidment NT, Ritz B, Bronstein JM. 2013. Aldehyde dehydrogenase inhibition as a pathogenic mechanism in Parkinson disease. Proc Natl Acad Sci U S A 110:636–641. https://doi.org/10.1073/pnas.1220399110.
118. Casida JE, Ford B, Jinsmaa Y, Sullivan P, Cooney A, Goldstein DS. 2014. Benomyl, aldehyde dehydrogenase, DOPAL, and the catecholaldehyde hypothesis for the pathogenesis of Parkinson's disease. Chem Res Toxicol 27:1359–1361. https://doi.org/10.1021/tx5002223.
119. Leiphon LJ, Picklo MJ. Sr, 2007. Inhibition of aldehyde detoxification in CNS mitochondria by fungicides. Neurotoxicology 28:143–149. https://doi.org/10.1016/j.neuro.2006.08.008.
120. Jakab A, Balla N, Ragyak A, Nagy F, Kovacs F, Sajtos Z, Toth Z, Borman AM, Pocsi I, Baranyai E, Majoros L, Kovacs R. 2021. Transcriptional profiling of the *Candida auris* response to exogenous farnesol exposure. mSphere 6:e0071021. https://doi.org/10.1128/mSphere.00710-21.
121. Nagy F, Vitalis E, Jakab A, Borman AM, Forgacs L, Toth Z, Majoros L, Kovacs R. 2020. *In vitro* and *in vivo* effect of exogenous farnesol exposure against *Candida auris*. Front Microbiol 11:957. https://doi.org/10.3389/fmicb.2020.00957.
122. Shirtliff ME, Krom BP, Meijering RA, Peters BM, Zhu J, Scheper MA, Harris ML, Jabra-Rizk MA. 2009. Farnesol-induced apoptosis in *Candida albicans*. Antimicrob Agents Chemother 53:2392–2401. https://doi.org/10.1128/AAC.01551-08.
123. Hasim S, Vaughn EN, Donohoe D, Gordon DM, Pfiffner S, Reynolds TB. 2018. Influence of phosphatidylserine and phosphatidylethanolamine on farnesol tolerance in *Candida albicans*. Yeast 35:343–351. https://doi.org/10.1002/yea.3297.
124. Machida K, Tanaka T, Fujita K, Taniguchi M. 1998. Farnesol-induced generation of reactive oxygen species via indirect inhibition of the mitochondrial electron transport chain in the yeast *Saccharomyces cerevisiae*. J Bacteriol 180:4460–4465. https://doi.org/10.1128/JB.180.17.4460-4465.1998.
125. Fairn GD, MacDonald K, McMaster CR. 2007. A chemogenomic screen in *Saccharomyces cerevisiae* uncovers a primary role for the mitochondria in farnesol toxicity and its regulation by the Pkc1 pathway. J Biol Chem 282:4868–4874. https://doi.org/10.1074/jbc.M610575200.
126. Yadav SK, Singla-Pareek SL, Ray M, Reddy MK, Sopory SK. 2005. Methylglyoxal levels in plants under salinity stress are dependent on glyoxalase I and glutathione. Biochem Biophys Res Commun 337:61–67. https://doi.org/10.1016/j.bbrc.2005.08.263.
127. Nahar K, Hasanuzzaman M, Alam MM, Fujita M. 2015. Glutathione-induced drought stress tolerance in mung bean: coordinated roles of the antioxidant defence and methylglyoxal detoxification systems. AoB Plants 7:plv069. https://doi.org/10.1093/aobpla/plv069.
128. Melvin P, Bankapalli K, D'Silva P, Shivaprasad PV. 2017. Methylglyoxal detoxification by a DJ-1 family protein provides dual abiotic and biotic stress tolerance in transgenic plants. Plant Mol Biol 94:381–397. https://doi.org/10.1007/s11103-017-0613-9.
129. Vemanna RS, Babitha KC, Solanki JK, Amarnatha Reddy V, Sarangi SK, Udayakumar M. 2017. Aldo-keto reductase-1 (*AKR1*) protect cellular enzymes from salt stress by detoxifying reactive cytotoxic compounds. Plant Physiol Biochem 113:177–186. https://doi.org/10.1016/j.plaphy.2017.02.012.
130. Mahmud JA, Hasanuzzaman M, Khan MIR, Nahar K, Fujita M. 2020. Beta-aminobutyric acid pretreatment confers salt stress tolerance in *Brassica napus* L. by modulating reactive oxygen species metabolism and methylglyoxal detoxification. Plants (Basel) 9.
131. Rohman MM, Islam MR, Monsur MB, Amiruzzaman M, Fujita M, Hasanuzzaman M. 2019. Trehalose protects maize plants from salt stress and phosphorus deficiency. Plants (Basel) 8.
132. Veena Reddy VS, Sopory SK. 1999. Glyoxalase I from *Brassica juncea*: molecular cloning, regulation and its over-expression confer tolerance in transgenic tobacco under stress. Plant J 17:385–395. https://doi.org/10.1046/j.1365-313x.1999.00390.x.
133. Shanks RM, Caiazza NC, Hinsa SM, Toutain CM, O'Toole GA. 2006. *Saccharomyces cerevisiae*-based molecular tool kit for manipulation of genes from gram-negative bacteria. Appl Environ Microbiol 72:5027–5036. https://doi.org/10.1128/AEM.00682-06.
134. Grahl N, Demers EG, Crocker AW, Hogan DA. 2017. Use of RNA-Protein complexes for genome editing in non-albicans *Candida Species*. mSphere 2:e00218-17. https://doi.org/10.1128/mSphere.00218-17.
135. Kim D, Paggi JM, Park C, Bennett C, Salzberg SL. 2019. Graph-based genome alignment and genotyping with HISAT2 and HISAT-

genotype. Nat Biotechnol 37:907–915. https://doi.org/10.1038/s41587-019-0201-4.
136. Liao Y, Smyth GK, Shi W. 2014. featureCounts: an efficient general purpose program for assigning sequence reads to genomic features. Bioinformatics 30:923–930. https://doi.org/10.1093/bioinformatics/btt656.
137. Robinson MD, McCarthy DJ, Smyth GK. 2010. edgeR: a Bioconductor package for differential expression analysis of digital gene expression data. Bioinformatics 26:139–140. https://doi.org/10.1093/bioinformatics/btp616.
138. Basenko EY, Pulman JA, Shanmugasundram A, Harb OS, Crouch K, Starns D, Warrenfeltz S, Aurrecoechea C, Stoeckert CJ, Jr, Kissinger JC, Roos DS, Hertz-Fowler C. 2018. FungiDB: an integrated bioinformatic resource for fungi and oomycetes. J Fungi (Basel) 4.
139. Stajich JE, Harris T, Brunk BP, Brestelli J, Fischer S, Harb OS, Kissinger JC, Li W, Nayak V, Pinney DF, Stoeckert CJ, Jr, Roos DS. 2012. FungiDB: an integrated functional genomics database for fungi. Nucleic Acids Res 40:D675–81.